

S-process: observations vs predictions

Roberto Gallino⁽¹⁾

Sara Bisterzo ^(1,2)

(1) Dipartimento di Fisica Generale, Università' di Torino, v. P. Giuria
1, 10025 Torino, Italy

(2) Forschungszentrum Karlsruhe, Institut für Kernphysik, Postfach 3640
D76021, Karlsruhe, Germany

The classical analysis

- Definition of s-process: in B²FH – [Merrill (1952) had seen Tc before].
- *Phenomenological approach*: see Clayton, D.D., Principles of stellar evolutions and nucleosynthesis, The University of Chicago press, 1968
- Based on the σN_s curve in the Solar System
- Two main results:
 - i) Multiple irradiations are needed to bypass the bottlenecks of nuclei with very small cross sections (neutron *magic* nuclei $N = 50, 82, 126$);
 - ii) Far from bottlenecks, steady flow conditions prevail where $\sigma N \sim \text{const.}$ (for unbranched nuclei).

Along the s path, the differential equation for the abundance of the heavy nuclei is:

$$\frac{dN(A)}{dt} = N(A-1)n_n \langle \sigma((A-1), v)v \rangle - N(A)n_n \langle \sigma(A, v)v \rangle \quad (1)$$

where $\langle \sigma(A, v)v \rangle$ indicates the Maxwellian averaged product of cross section and relative velocity, and n_n is the neutron density. Let us replace time with the time integrated neutron flux, or *neutron exposure* τ :

$$\tau = \int_0^t n_n v_T dt \quad \text{mbarn}^{-1}$$

(here v_T is the thermal velocity). With $\bar{\sigma}(A)$ denoting the ratio $\langle \sigma(A, v)v \rangle / v_T$, one has:

$$\frac{dN(A)}{d\tau} = N(A-1)\bar{\sigma}(A-1) - N(A)\bar{\sigma}(A) \quad (2)$$

which in steady state conditions yields $\bar{\sigma}(A)N(A) = \text{const.}$

If: $\rho(\tau) = \frac{f N_{56}}{\tau_0} e^{-\frac{\tau}{\tau_0}}$, (exponential distribution of exposures: Main Component)

Then: $\sigma(A)N_s(A) = f N_{56} \tau_0 \prod_{A_i=56}^A [1 + (\sigma(A_i)\tau_0)^{-1}]^{-1}$

Branchings along the s-path

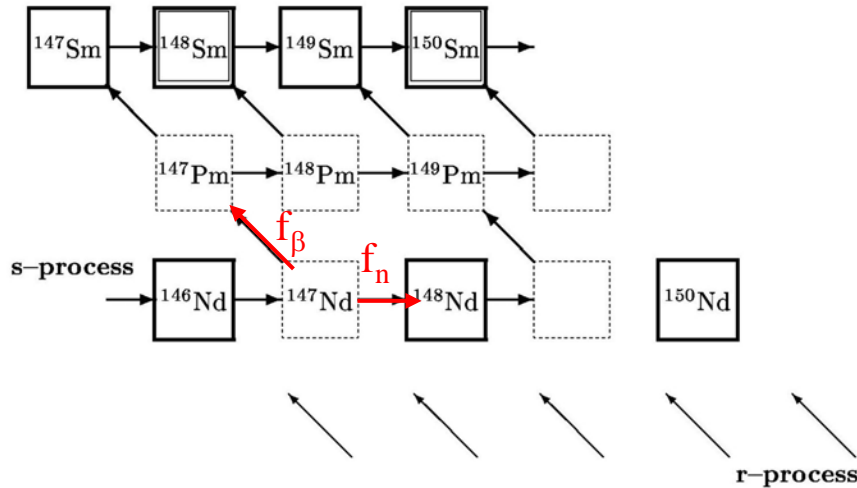


Fig. 1. The s-process path in the Nd/Pm/Sm-region

Example: ^{147}Nd

$$\lambda_{\beta} = 1 / \tau_{\beta}$$

$$\lambda_n = N_n \langle \sigma v \rangle$$

$$f_{\beta} = \lambda_{\beta} / (\lambda_{\beta} + \lambda_n)$$

$$f_n = \lambda_n / (\lambda_{\beta} + \lambda_n)$$

$$(f_{\beta} + f_n = 1)$$

- Reaction Branchings (Clayton & Ward 1974): β -decay competes with n-capture, branching ratios f_{β} and abundances inform on (T, n_n) conditions in the parent star.
- Branching analysis yielded conditions $\sim 30\text{KeV}$ and $n_n \sim 5 \times 10^8 \text{ cm}^{-3}$.

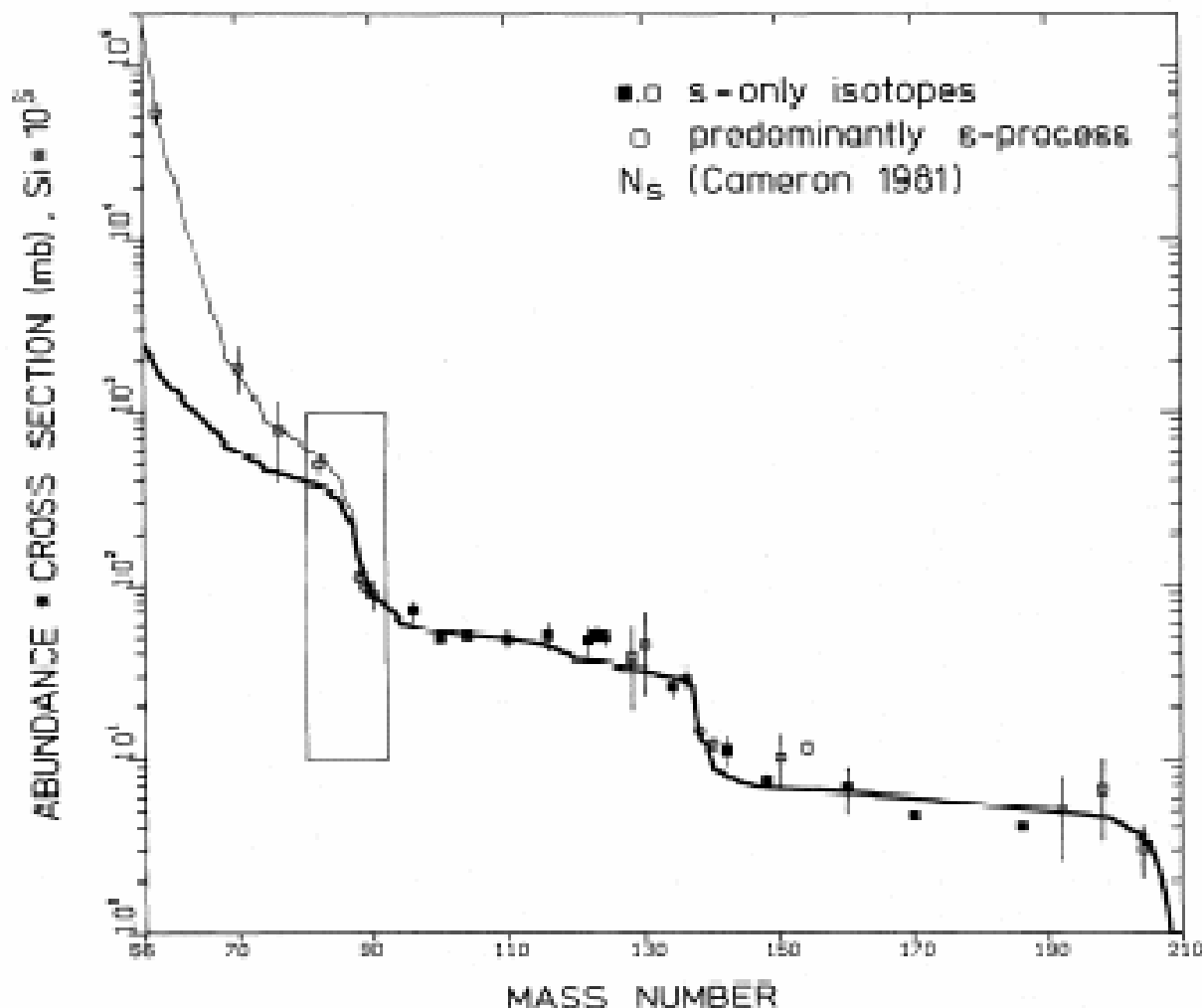


FIG. 2.—The product of *s*-process abundance times cross section as a function of mass number. The symbols correspond to empirical values for *s*-only isotopes (squares) or to neutron magic isotopes which are predominantly produced by the *s*-process (circles). The respective abundances are taken from the solar abundance table of Cameron (1981). Error bars include the cross section uncertainties only. The calculated solid lines correspond to the strong and weak component in the exponential neutron fluence distribution.

How many s-process components?

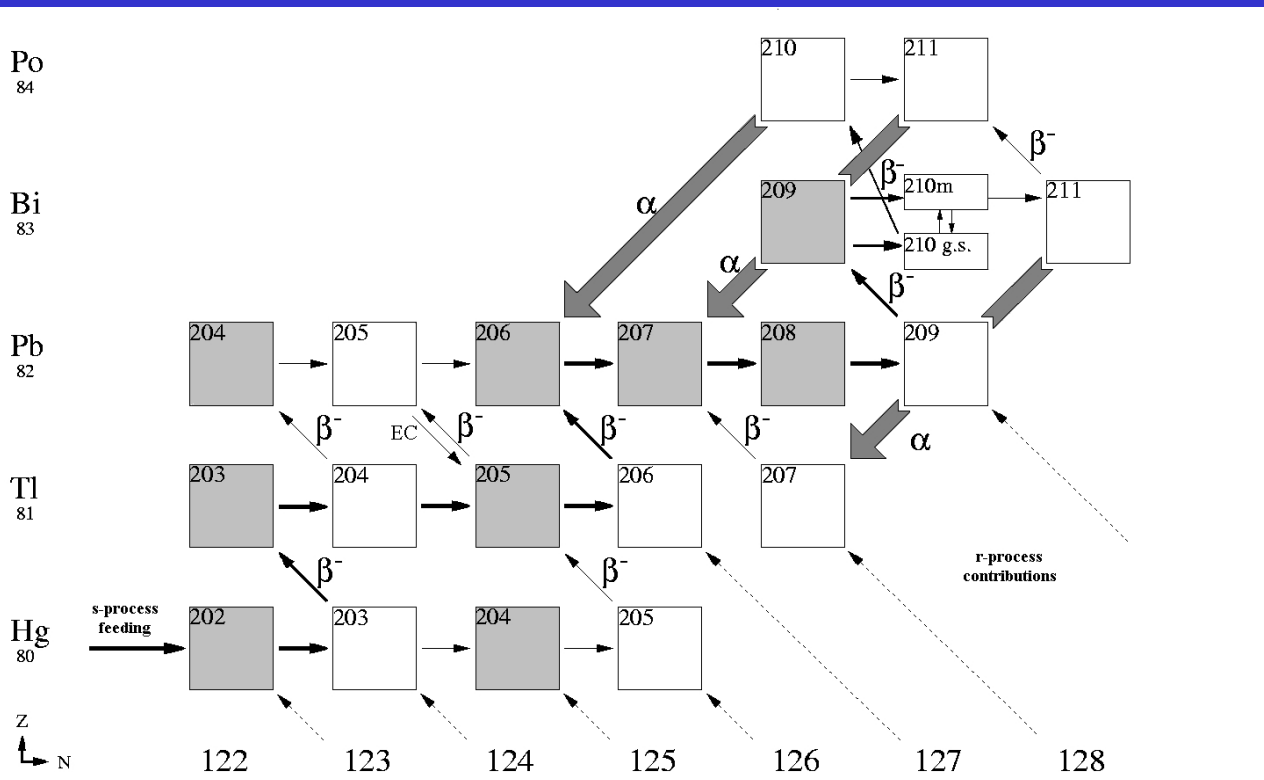
Three s-process components were anticipated by the classical analysis (Clayton and Rassbach 1974; Käppeler et al. 1982):

the weak ($A < 90$), the main, and the strong s-component (needed for reproducing $\sim 50\%$ of ^{208}Pb).

The main s-component is the outcome of many generations of Asymptotic Giant Branch stars (AGB) polluting the interstellar medium before the solar system formed.

Actually, the main s-component is far from being a unique process, depending on the efficiency of the so-called C13-pocket, the initial mass, and metallicity.

Termination of the s-process



^{208}Pb and ^{209}Bi

are at the
termination point
of the
s-fluence

(Ratzel et al. PRC
70 065803 2004)

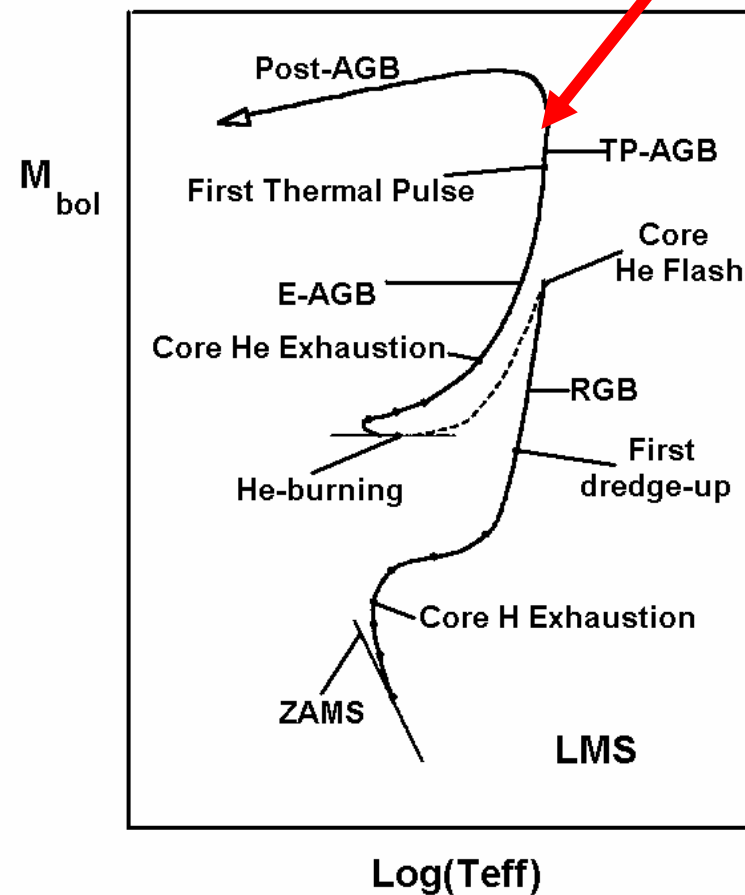
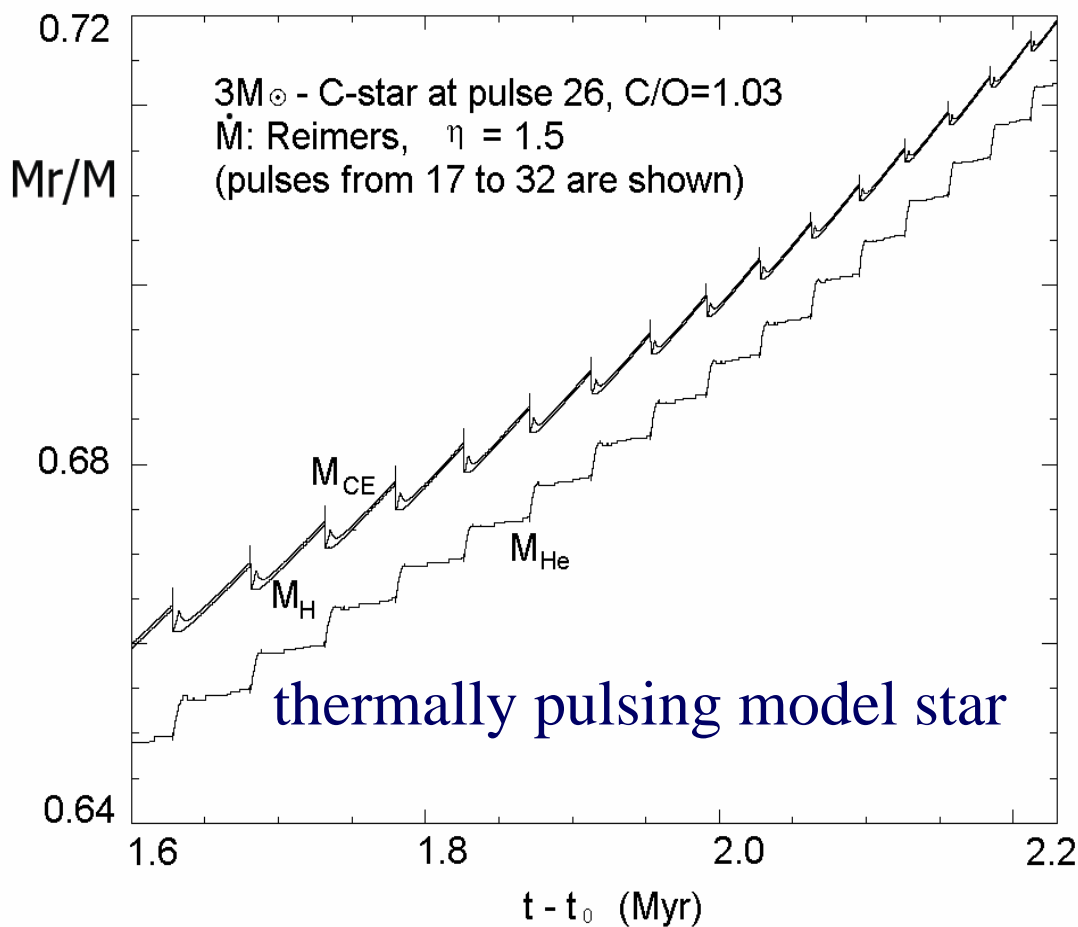
With a primary-like ^{13}C -pocket, lead becomes the major
s-process product at low metallicity

S-process in AGB stars

- AGB stars and the two sources of neutrons
- The choice of ^{13}C -pocket guided by observations
- Lead stars at low metallicities
- Primary light elements
- Lead stars with s and r-process enhancements
- The Sr, Y, Zr, problem and choice of the initial mass
- Na and choice of the initial mass
- C-rich and no s-process rich AGB stars

Low-mass thermally pulsing stars

Envelope loss by stellar winds



(Straniero et al. 1997; Busso et al. 1999)

TP: thermal pulses

N-capture nucleosynthesis during the interpulse: the ^{13}C pocket

Straniero et al. 1995,
Gallino et al. 1998

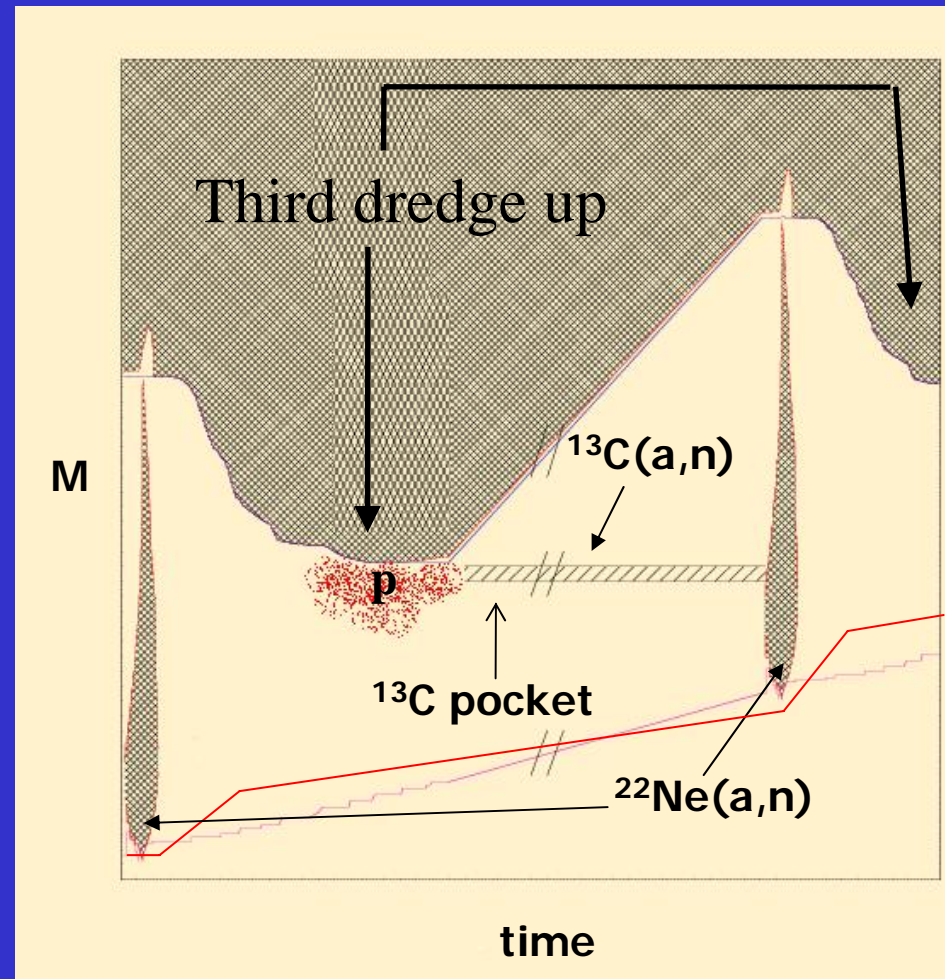
Neutron source:
 $^{12}\text{C}(p,\gamma)^{13}\text{N}(\beta^+)^{13}\text{C}(\alpha,n)$.

Type: **primary**

When: interpulse $T_6 > 90$.

Where: He-intershell zone

Density: 10^7 (neutrons/cm 3)



The two alternate neutron sources in AGB stars



Needs ^{13}C

Major neutron source

^{13}C -pocket

Primary source!

$T_8 = 0.9-1$

Interpulse phase

$(1-0.4) \times 10^5 \text{ yr}$

Radiative conditions

$N_n \sim 10^7 \text{ cm}^{-3}$



Abundant ^{22}Ne

Minor neutron source

Neutron burst

Secondary source

$T_8 \leq 3$ (low ^{22}Ne efficiency)

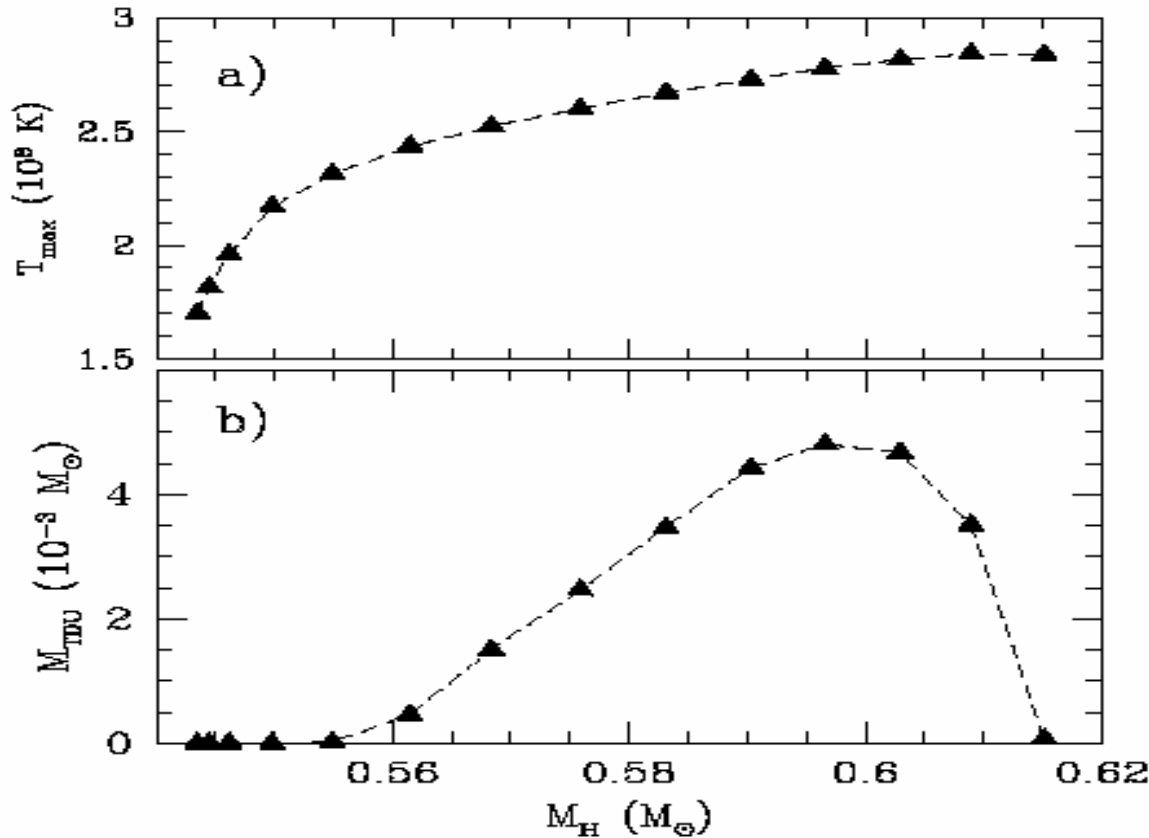
Thermal pulse

$\sim 6 \text{ yr}$

Convective conditions

$N_n (\text{peak}) \sim 10^{10} \text{ cm}^{-3}$

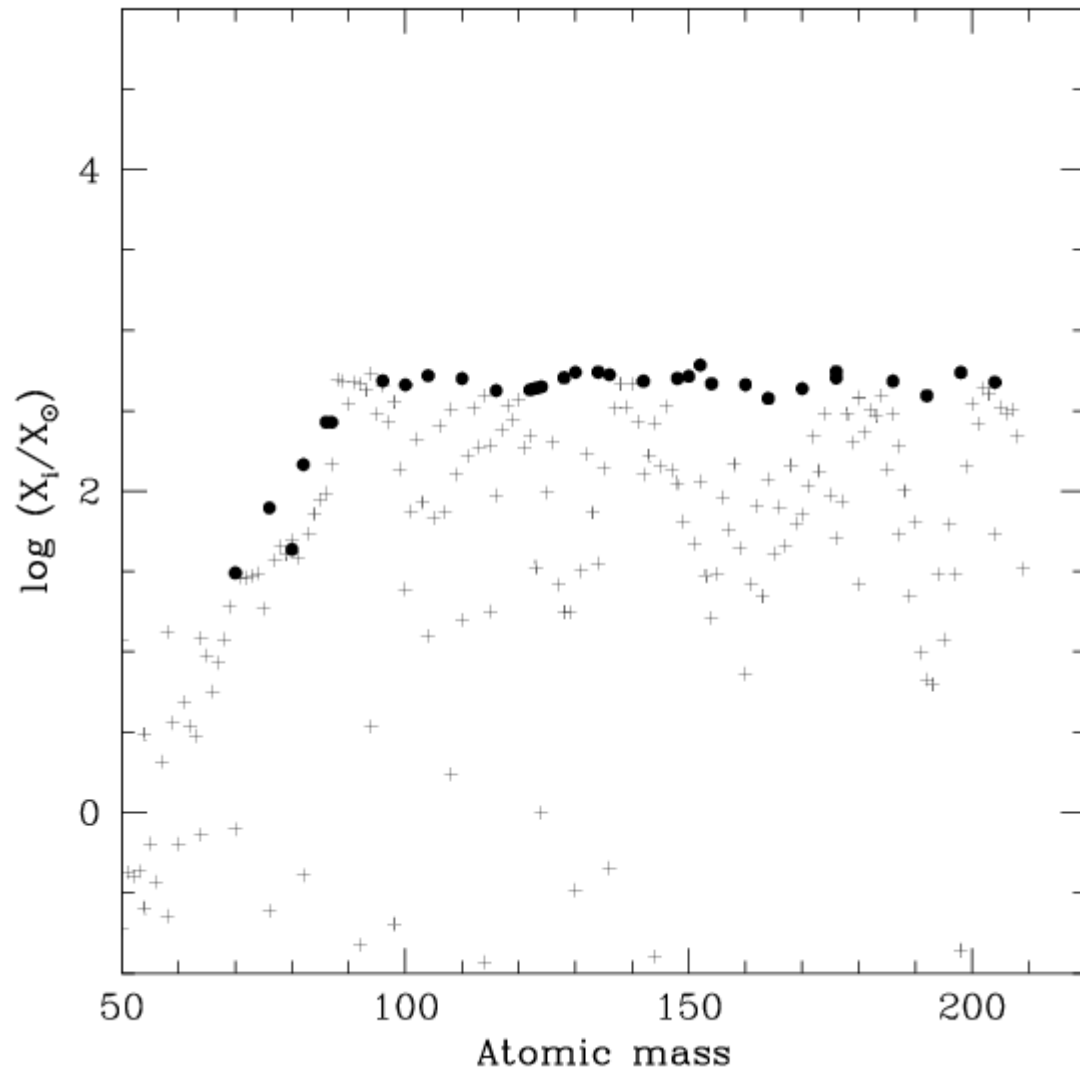
a) Maximum temperature in subsequent He-flashes



Straniero et al. 2006
astro-ph/0501405
(Nucl. Phys. A,
Special Volume on
Nuclear Astrophysics,
ed. K. Langanke, M.
Wiescher and F. -K.
Thielemann, in press)

b) Third dredge-up mass per pulse

Reproduction of the Solar Main Component (Gallino et al. 1998)



^{13}C -pocket choice:

- artificially introduced
- ad hoc modulated
- constant Pulse by Pulse

AND METALLICITY

$$[\text{Fe}/\text{H}] = -0.3$$

Tools for model tests through observations

Extensive tests started in the early 80's. Often only 'average' abundance parameters could be obtained with sufficient precision.

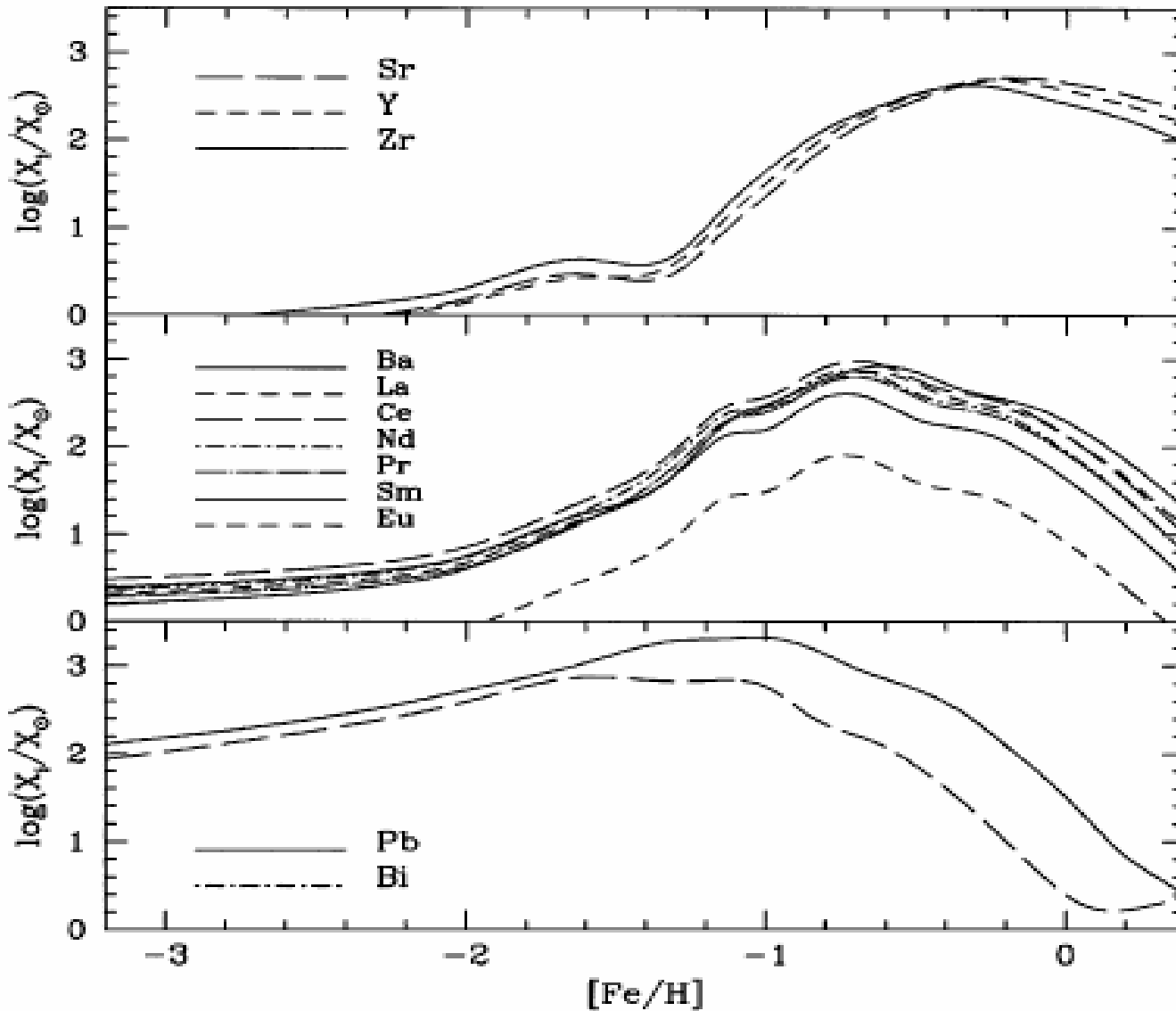
[hs/Fe]: average logarithmic abundance of 'heavy s-elements' (Ba-peak) with respect to the Sun; [ls/Fe] for 'light s' (Y, Zr).

$$[\text{hs/Fe}] = \log\{1/4(\text{Ba}+\text{La}+\text{Nd}+\text{Sm})/(\text{Fe})\}_{*-} - \log\{1/4(\text{Ba}+\text{La}+\text{Nd}+\text{Sm})/(\text{Fe})\}_{\odot}$$

$$[\text{ls/Fe}] = \log\{1/2(\text{Y}+\text{Zr})/(\text{Fe})\}_{*-} - \log\{1/2(\text{Y}+\text{Zr})/(\text{Fe})\}_{\odot}$$

$$[\text{hs/ls}] = \log\{(\text{Ba}+\text{La}+\text{Nd}+\text{Sm})/(\text{Y}+\text{Zr})\}_{*-} - \log\{(\text{Ba}+\text{La}+\text{Nd}+\text{Sm})/(\text{Y}+\text{Zr})\}_{\odot}$$

Solar system main component: [hs/ls] \sim - 0.2



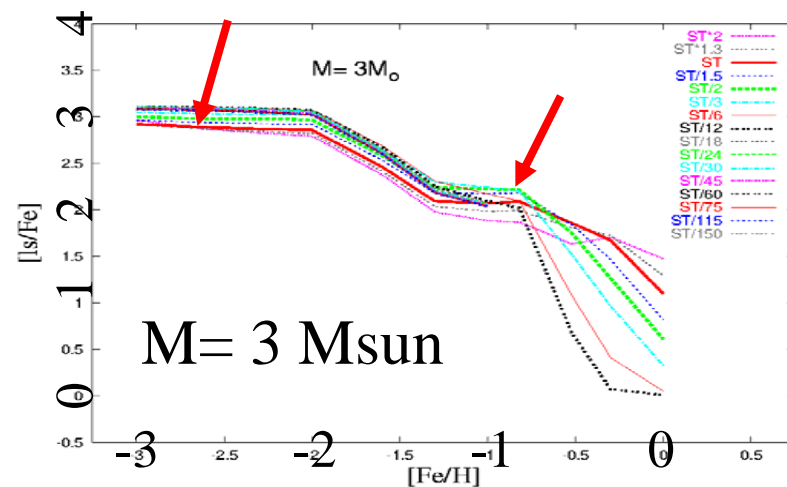
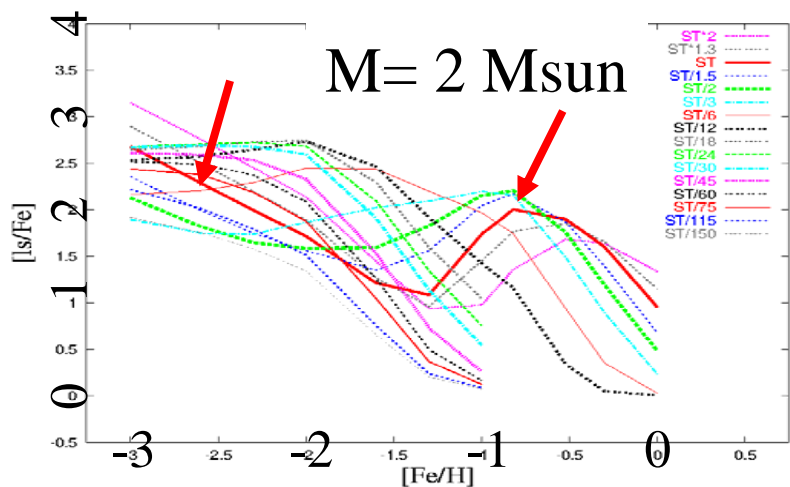
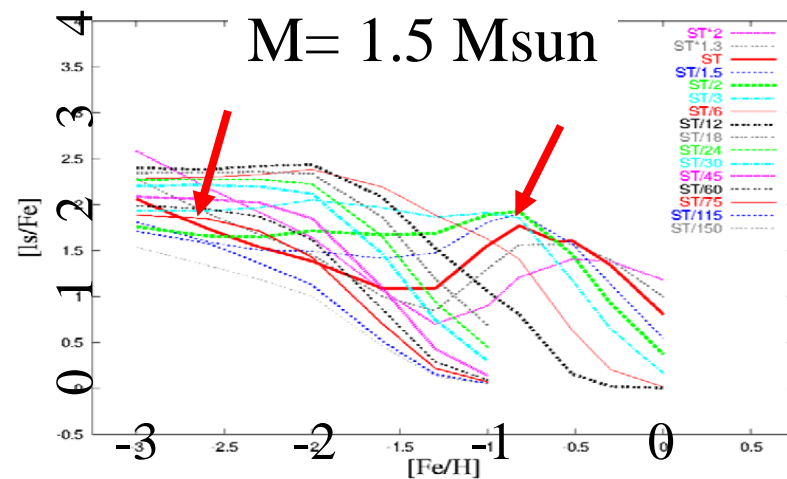
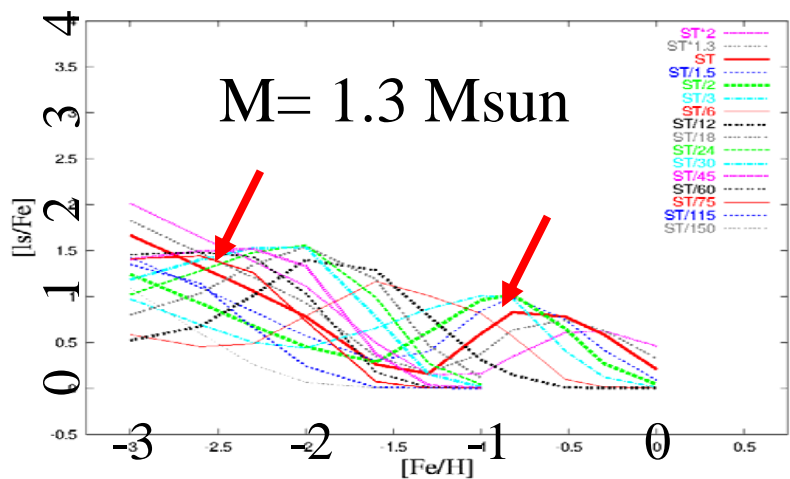
CASE ST

Metallicity dependence of the s-process distribution, seen through the abundance of the three s-peaks

Busso, Gallino, Wasserburg, ARAA 1999

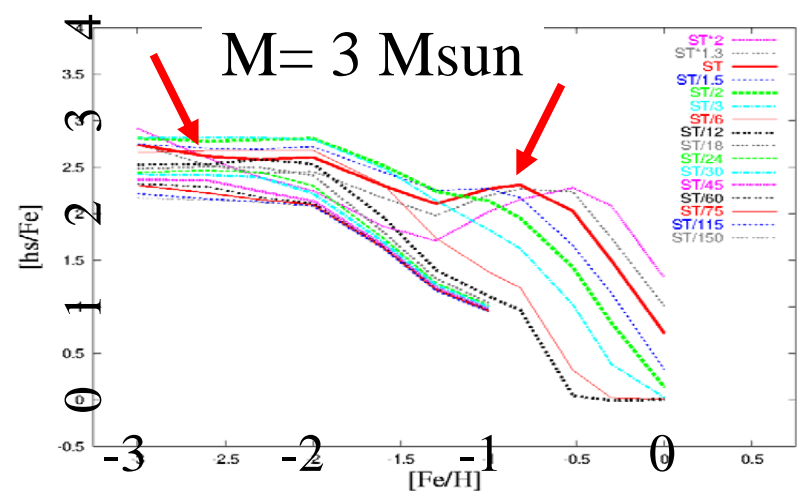
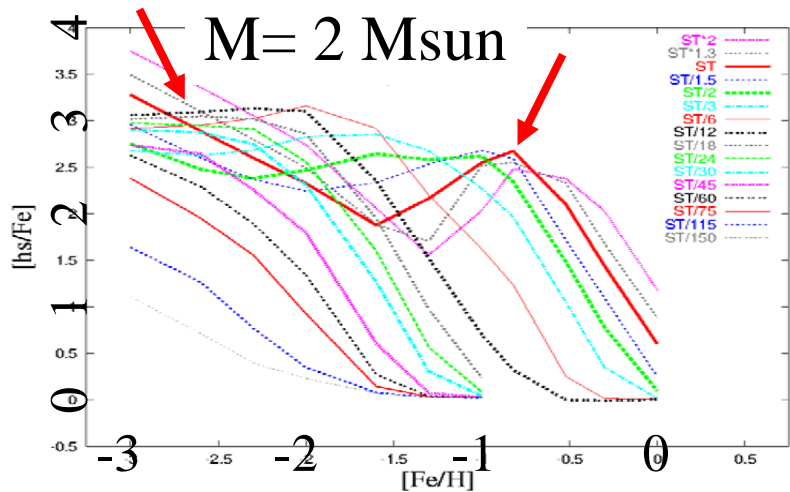
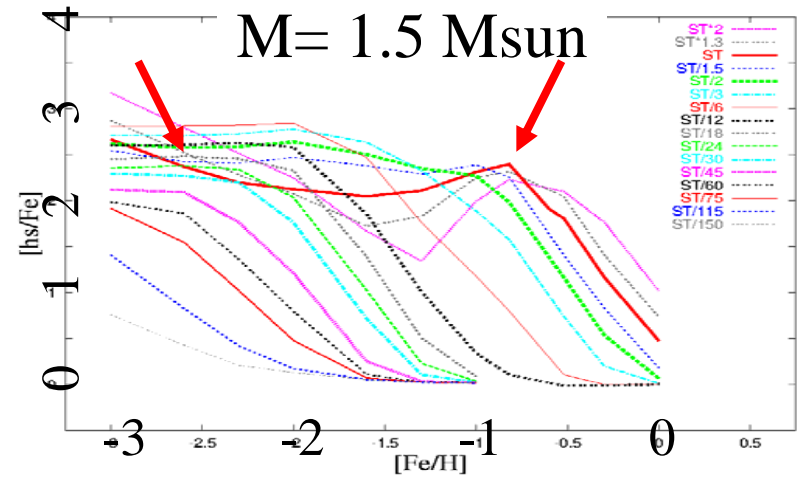
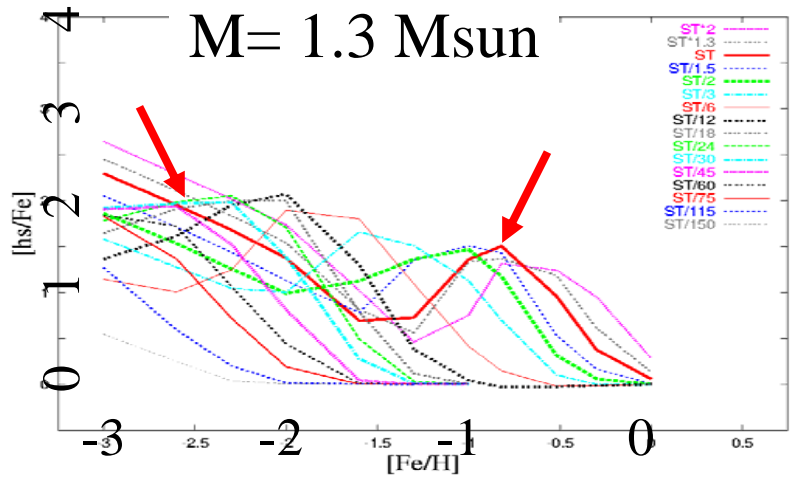
[ls/Fe] versus [Fe/H]

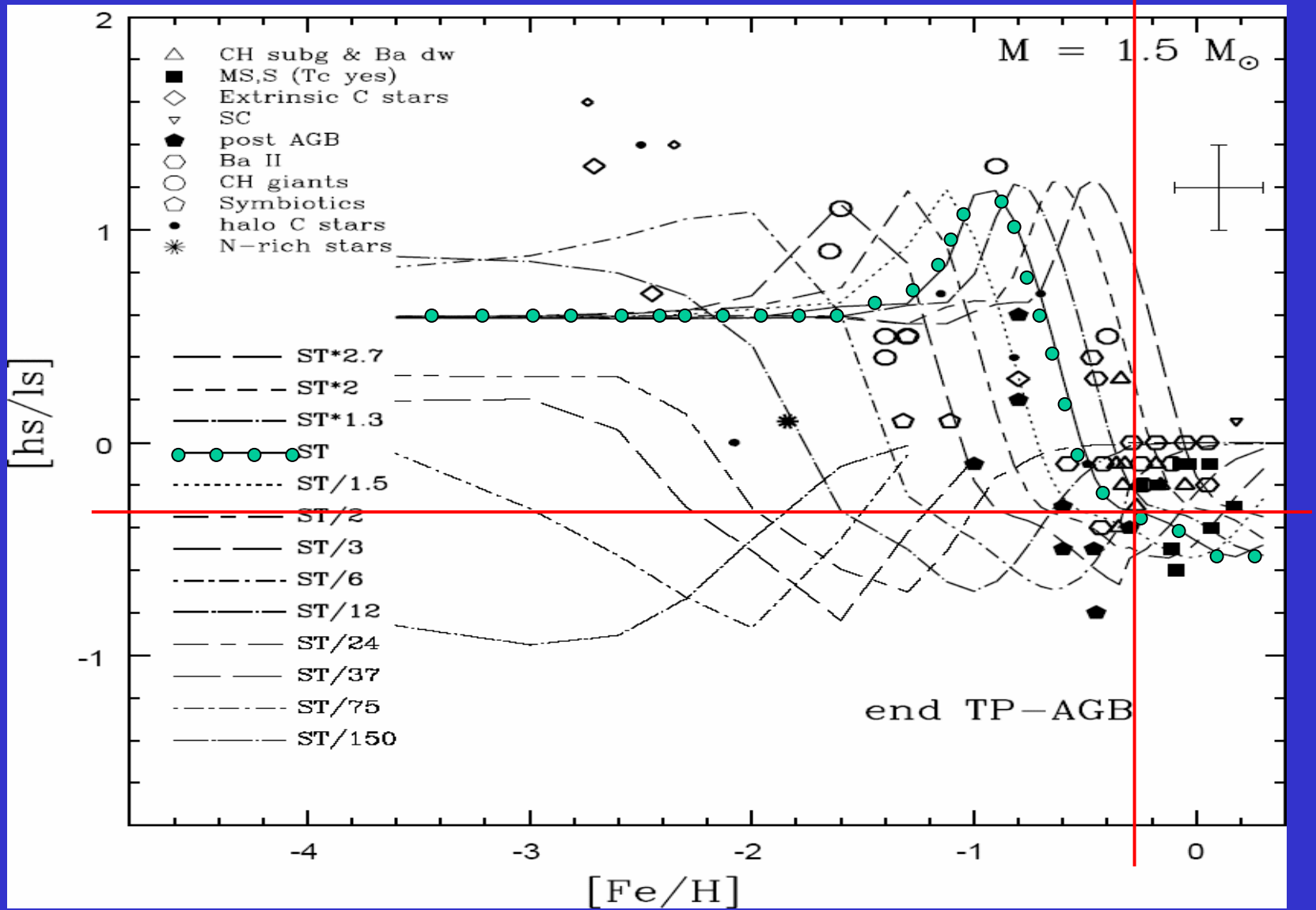
ls = $\langle Y, Zr \rangle$



[hs/Fe] versus [Fe/H]

hs = $\langle \text{Ba, La, Nd, Sm} \rangle$



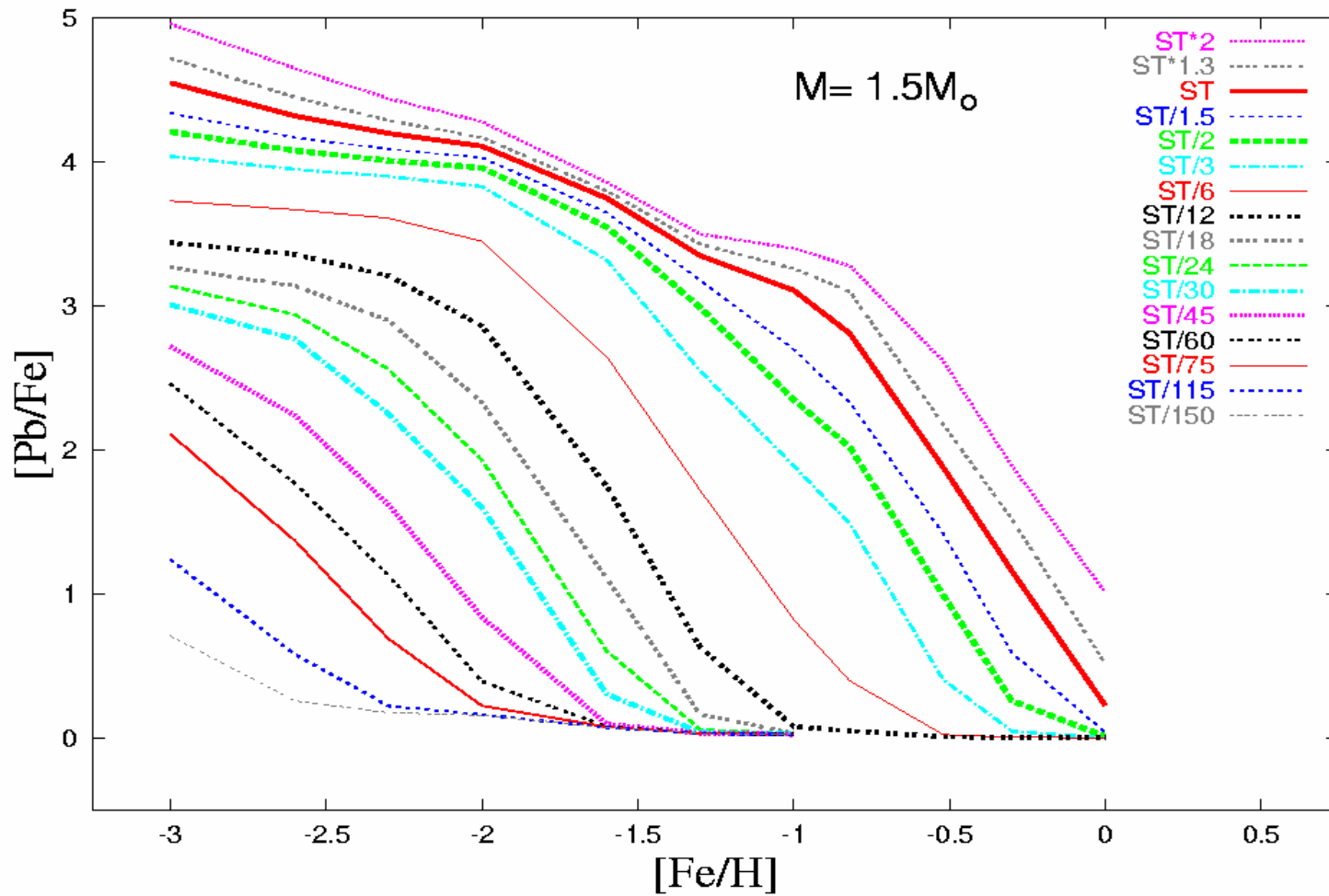


Busso et al. 2001 ApJ 557, 802

The Lead stars in the Halo

- Lead stars (C, s, Pb rich)
- C and s+r rich Lead stars
- s-enhanced stars and Pb predictions
- Nb: indicator of an extrinsic AGB in a binary system
- Na (and Mg): permits an estimate of the initial AGB stellar mass.

[Pb/Fe] vs [Fe/H] envelope last pulse condition



A. Intrinsic Halo AGBs

Today, the typical mass of an intrinsic AGB HALO STAR is $\sim 0.6 M_{\text{sun}}$ (initial mass 0.8 – 0.9 M_{sun}): NO TDU \rightarrow No C or s-process enrichment observable.

B. Extrinsic Halo AGBs (Dwarfs - Giants)

Accretion in Binaries (wind or Roche lobe overflow?)



Most of the halo C- s-rich stars probably belong to wide binary systems ($P \sim 2-3 \text{ yr}$)

t=0 (13 Gyr ago)



t=0.05-2 Gyr



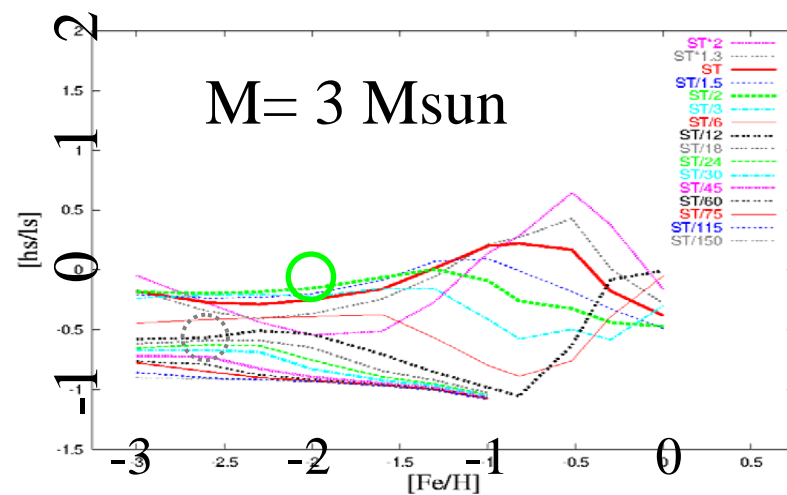
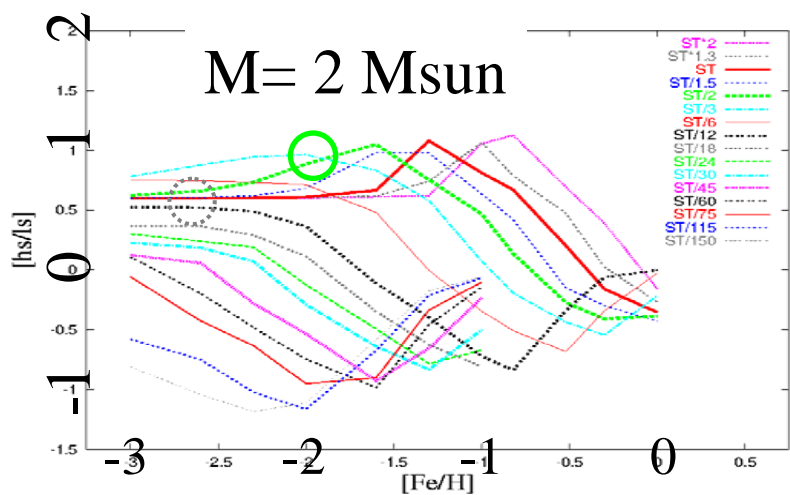
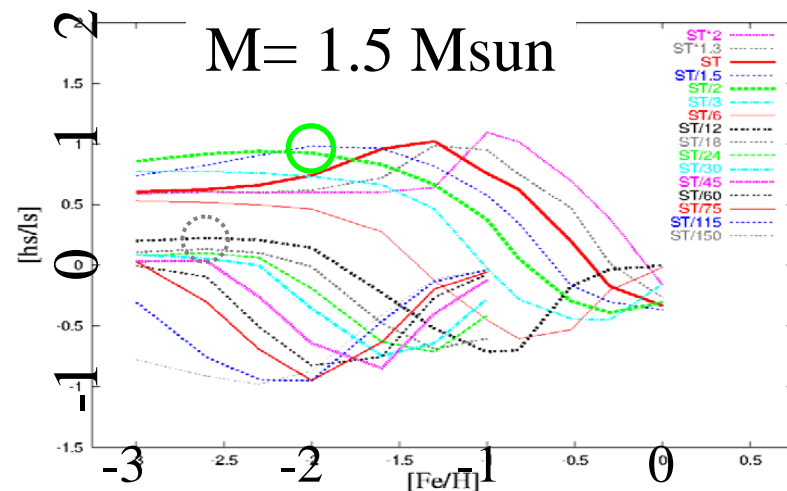
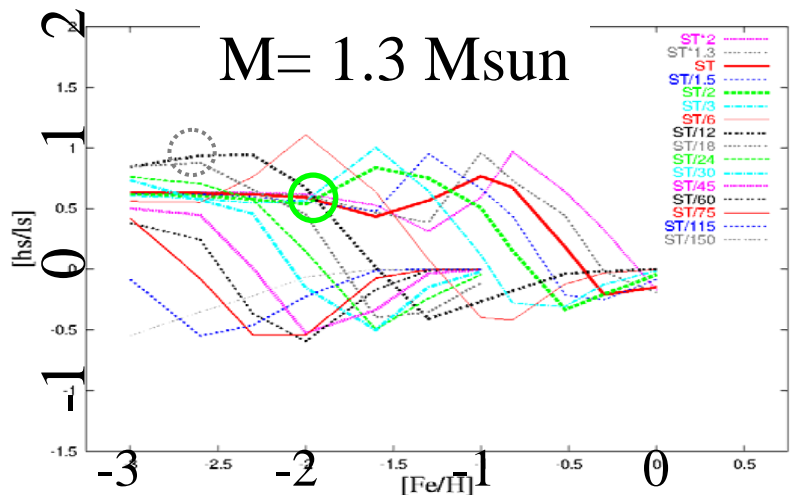
t=13 Gyr (now)



[hs/ls] versus [Fe/H]

○ Example: ST/12 at [Fe/H] = -2.5

○ Example: ST/2 at [Fe/H] = -2



Lead stars	[Fe/H]	T _{eff} (K)	log g	[Pb/Fe]	[ls/Fe]	[hs/Fe]	[hs/ls]	[Pb/hs]	M/M _o	¹³ C-pocket	dil	[Eu/Fe]	ref
CS 22183-015	-3.12	5200	2.5	3.17	0.54	1.78	1.24	1.39	1.3	ST/15	0.00	1.5*	1
CS 22880-074	-1.93	5850	3.8	1.90	0.16	1.19	1.03	0.71	1.2	ST/10	0.30	0.0*	2
CS 22898-027	-2.26	6250	3.7	2.84	0.87	2.17	1.30	0.67	1.3	ST/12	0.00	2.0*	2
CS 22942-019	-2.64	5000	2.4	≤ 1.6	1.64	1.51	-0.13	≤ 0.09	1.5	ST/75	0.00	0.5*	2
CS 29497-030	-2.70	6650	3.5	3.55	1.07	2.04	0.97	1.51	1.3	ST*2	0.40	0.5*	3
	-2.57	7000	4.1	3.65	1.19	2.23	1.04	1.42	1.3	ST*1.3	0.00	2.0*	10
CS 29526-110	-2.38	6500	3.2	3.30	1.11	1.94	0.83	1.36	1.3	ST/6	0.00	1.5*	2
CS 30301-015	-2.64	4750	0.8	1.70	0.29	1.10	0.81	0.60	1.3	ST/24	1.00	0.0*	2
CS 31062-012	-2.55	6250	4.5	2.40	0.59	1.93	1.34	0.47	1.3	ST/30	0.00	1.5*	2
CS 31062-050	-2.31	5600	3.0	2.90	1.02	2.28	1.26	0.62	1.3	ST/12	0.00	1.8*	2
	-2.42	5500	2.7	2.81	0.67	2.22	1.55	0.59	1.3	ST/12	0.00	1.8*	4
LP 625-44	-2.70	5500	2.5	2.60	1.26	2.33	1.07	0.27	1.3	ST/30	0.00	1.8*	5
HD 196944	-2.25	5250	1.8	1.90	0.61	0.91	0.30	0.99	1.5	ST/3	1.80	0.0*	2
	-2.40	5250	1.7	2.10	0.60	0.77	0.17	1.33	1.5	ST/3	1.3	0.5	6
HD 26	-1.25	5170	2.2	2.00	0.90	1.63	0.73	0.37	1.5	ST/2	0.80	0.5	6
HD 187861	-2.30	5320	2.3	3.30	1.30	1.97	0.67	1.33	1.5	ST/2	0.25	0.5	6
HD 189711	-1.80	3500	0.5	0.90	1.00	1.60	0.60	-0.70	1.3	ST/24	0.40	0.5	6
HD 198269	-2.20	4800	1.3	2.40	0.40	1.33	0.93	1.07	1.2	ST/9	0.40	0.5	6
HD 201626	-2.10	5190	2.3	2.60	0.90	1.60	0.70	1.00	1.5	ST/3	0.70	0.5	6
HD 224959	-2.20	5200	2.3	3.10	1.00	2.07	1.07	1.03	1.5	ST/2	0.35	0.5	6
V-Ari	-2.40	3580	-0.2	1.20	1.10	1.60	0.50	-0.40	1.2	ST/30	0.05	0.5	6
HE 0024-2523	-2.70	6625	4.3	3.30	1.07	1.63	0.57	1.67	1.3	ST/12	0.00	0.0*	7
HE 2148-1247	-2.30	6380	3.9	3.12	1.15	2.25	1.10	0.87	1.3	ST/12	0.00	2.0*	8
CS 22948-27	-2.47	4800	1.8	2.72	1.00	2.27	1.27	0.45	1.3	ST/24	0.25	1.5*	9
CS 29497-34	-2.90	4800	1.8	2.95	1.10	2.08	0.98	0.87	1.5	ST/4	1.00	1.5*	9
HE 0338-3945	-2.42	6160	4.1	3.10	1.02	2.31	1.30	0.79	1.3	ST/12	0.00	2.0*	11

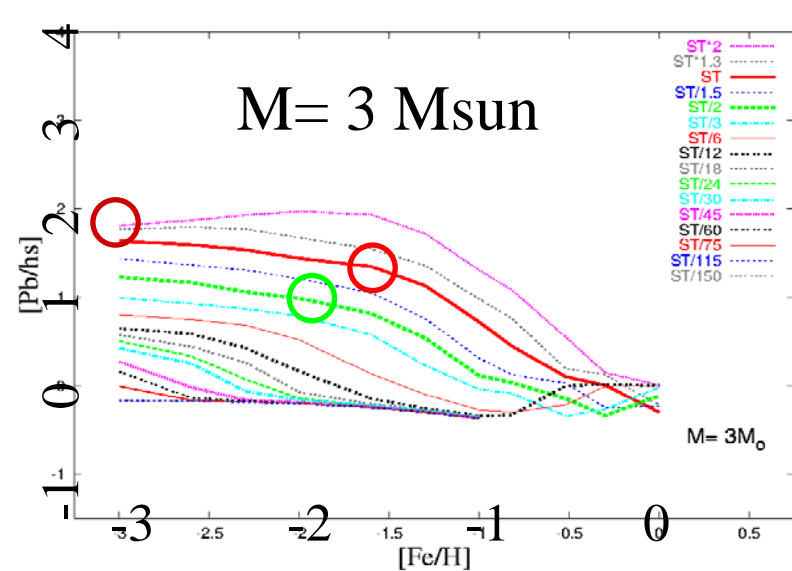
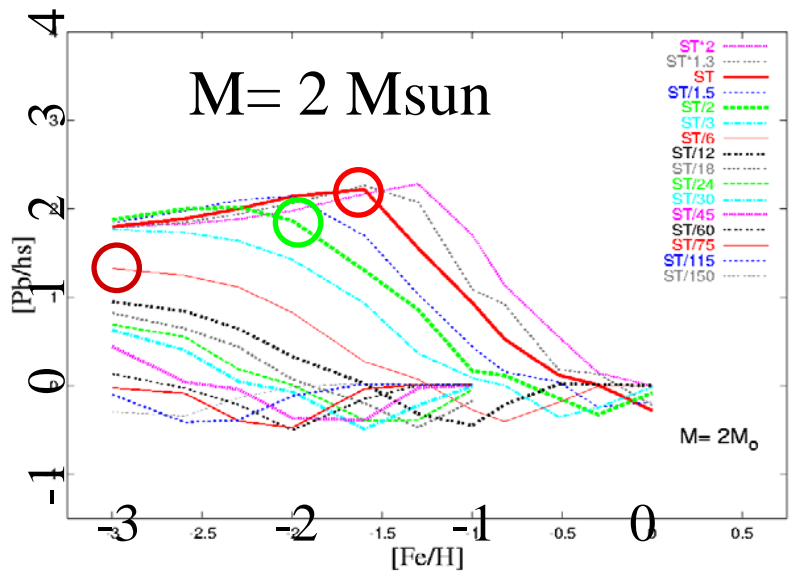
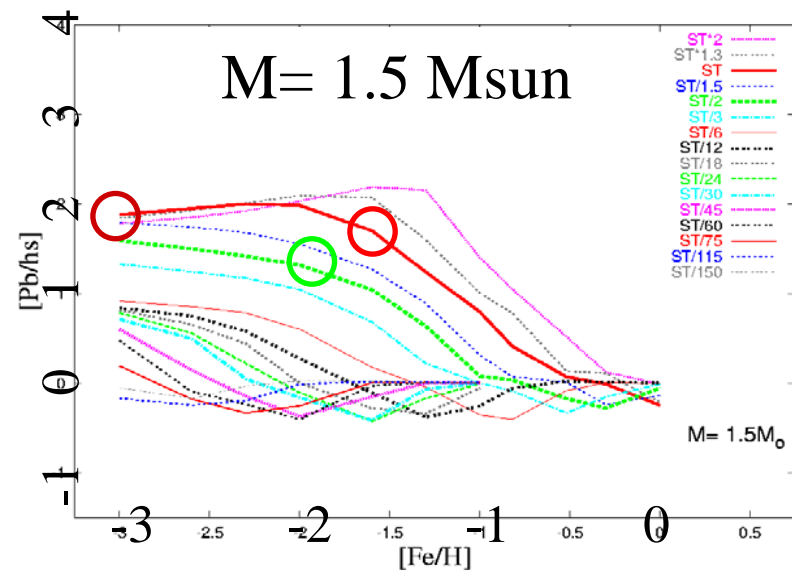
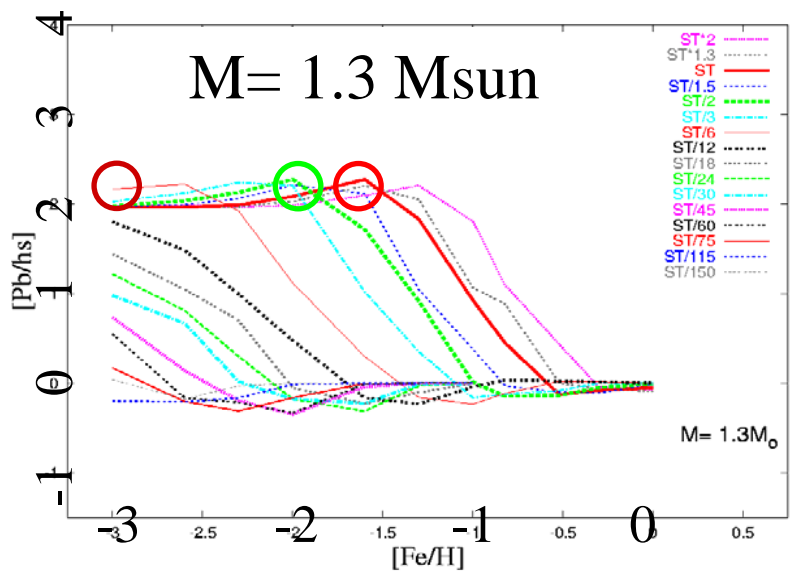
R-enriched stars

1. J. A. Johnson, M. Bolte, ApJ 579, L87 (2002)
2. W. Aoki, et al., ApJ 580, 1149 (2002)
3. T. Sivarani, et al., A&A 413, 1073 (2004)
4. J. A. Johnson, M. Bolte, ApJ 605, 462 (2004)
5. W. Aoki, et al., PASJ 54, 427 (2002)
6. S. Van Eck et al., A&A 404, 291 (2003)

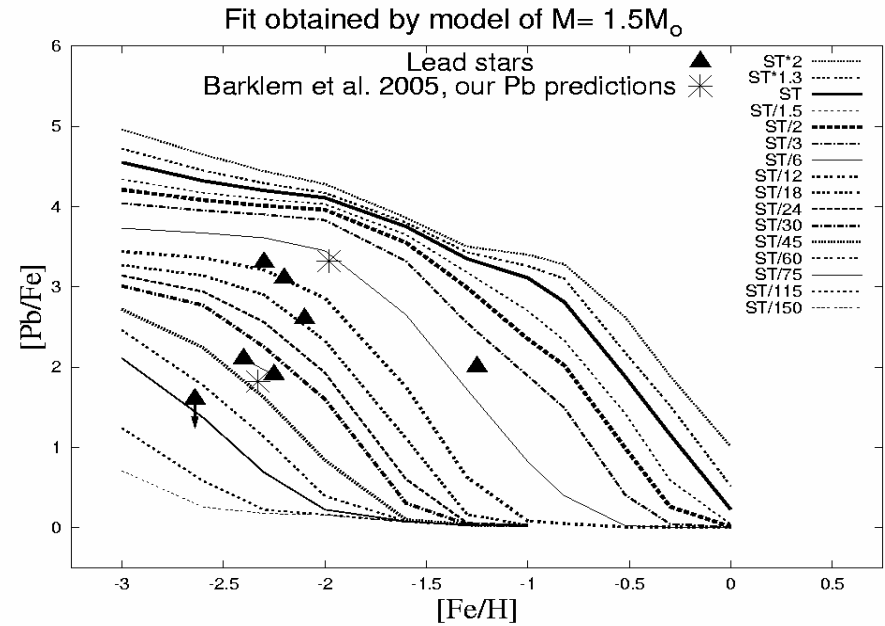
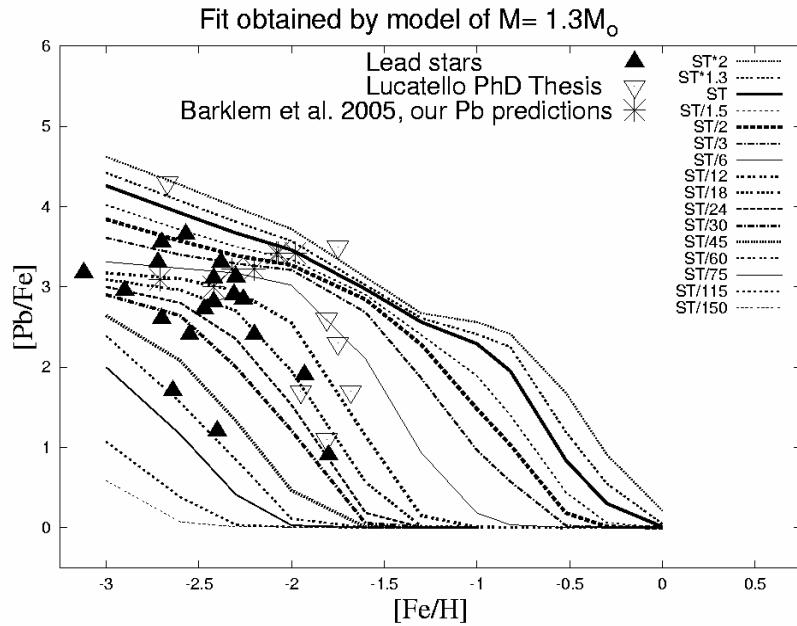
7. S. Lucatello, et al., AJ 125, 875 (2003)
8. J. G. Cohen et al., ApJ 588, 1082 (2003)
9. B. Barbuy, et al., A&A 429, 1031 (2005)
10. I. Ivans et al., ApJ 627, 145 (2005)
11. K. Jonsell et al., [astro-ph/0601476](https://arxiv.org/abs/astro-ph/0601476)

- 1- Lead stars (C, s, Pb rich)
- 2 – C and s+r rich Lead stars

[Pb/hs] versus [Fe/H]

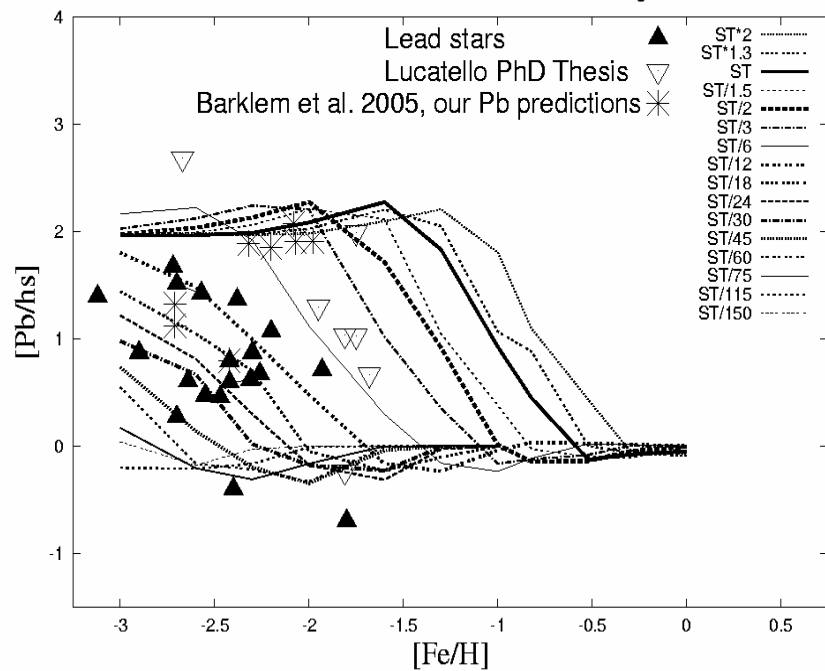


[Pb/Fe] versus [Fe/H]

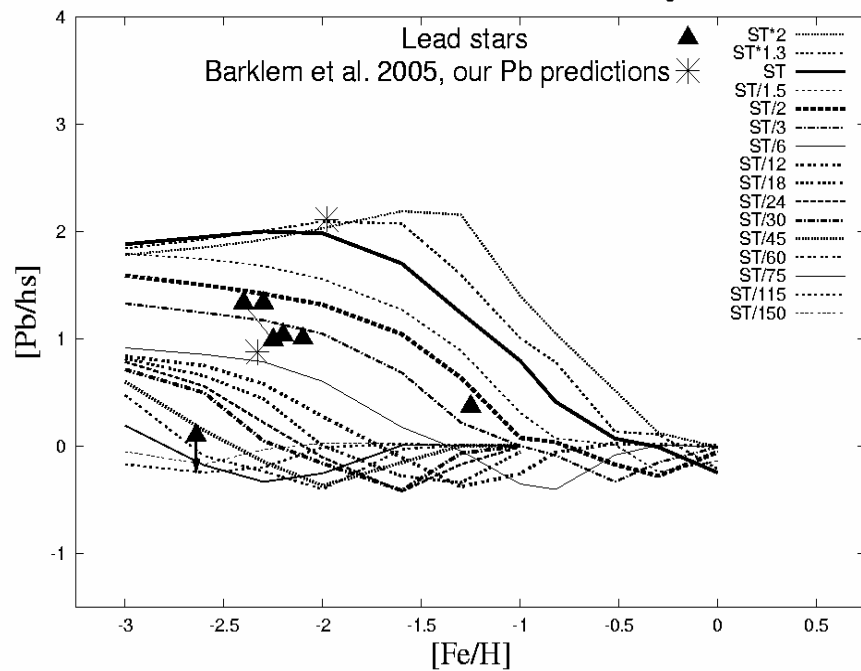


[Pb/hs] versus [Fe/H]

Fit obtained by model of $M= 1.3M_{\odot}$

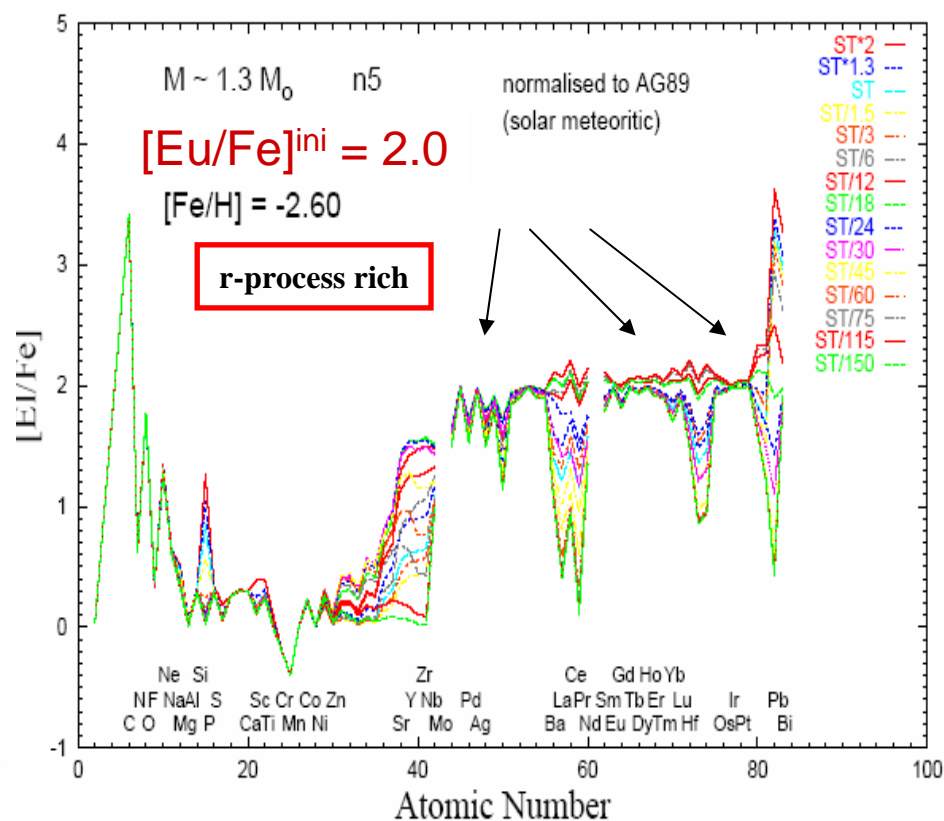
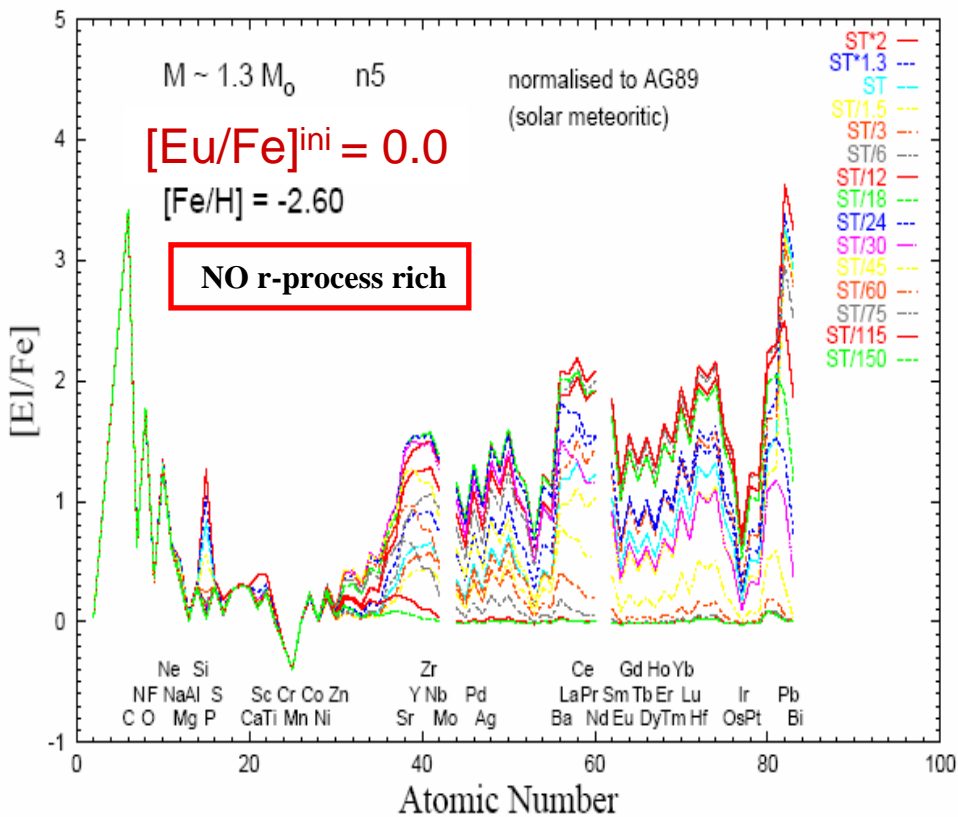


Fit obtained by model of $M= 1.5M_{\odot}$



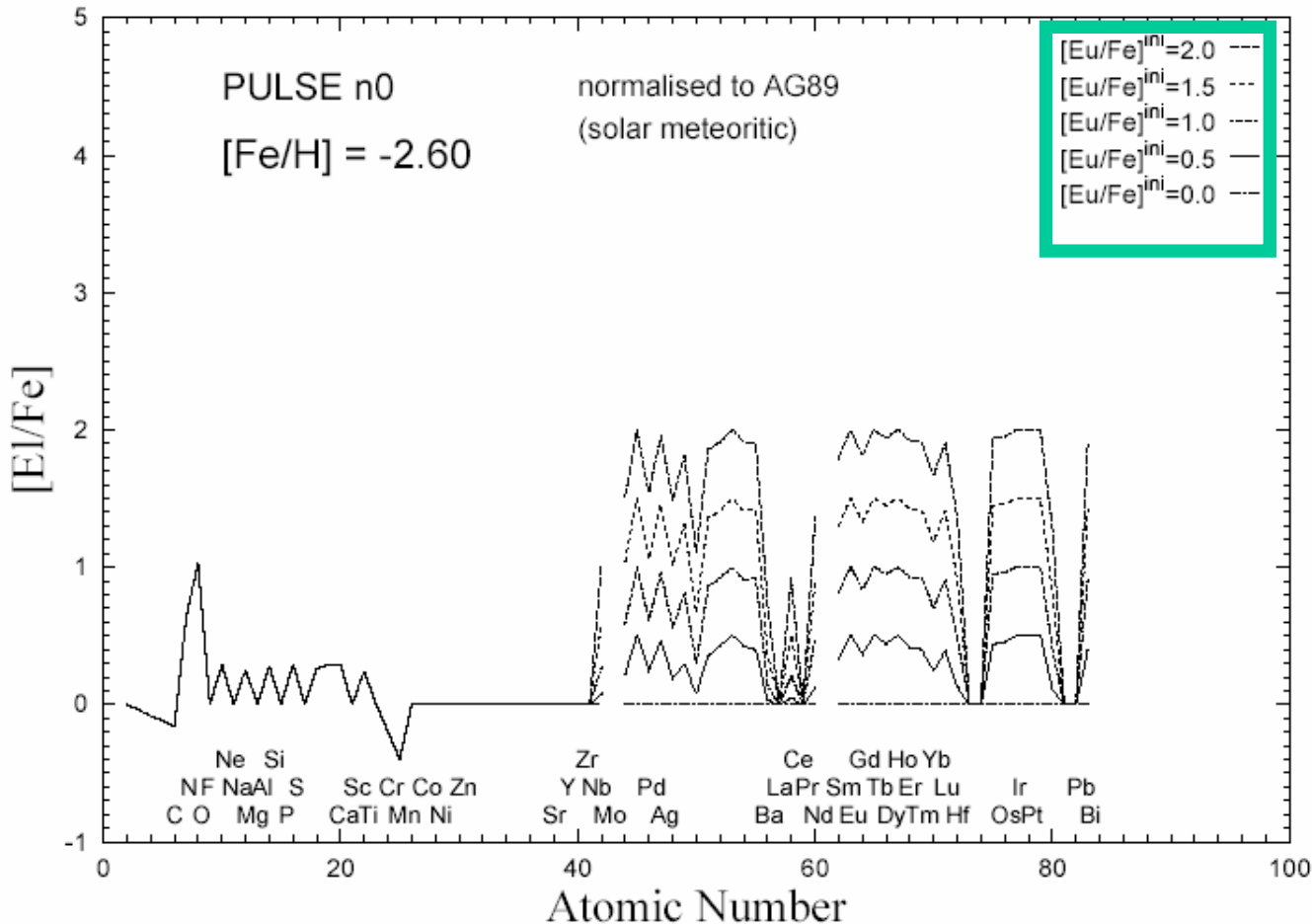
Effect of pre r-enrichment in s-enhanced stars

AGB star model of $M = 1.3 M_{\text{sun}}$ with $[\text{Fe}/\text{H}] = -2.60$.



Model with pre r-enrichment normalized to $[\text{Eu}/\text{Fe}]^{\text{ini}} = 2.0$ in the parental cloud: the envelope abundances in these stars are predicted by mass transfer from the more massive AGB companion in a binary system which formed from a parental cloud already enriched in r elements.

Choice of initial abundances



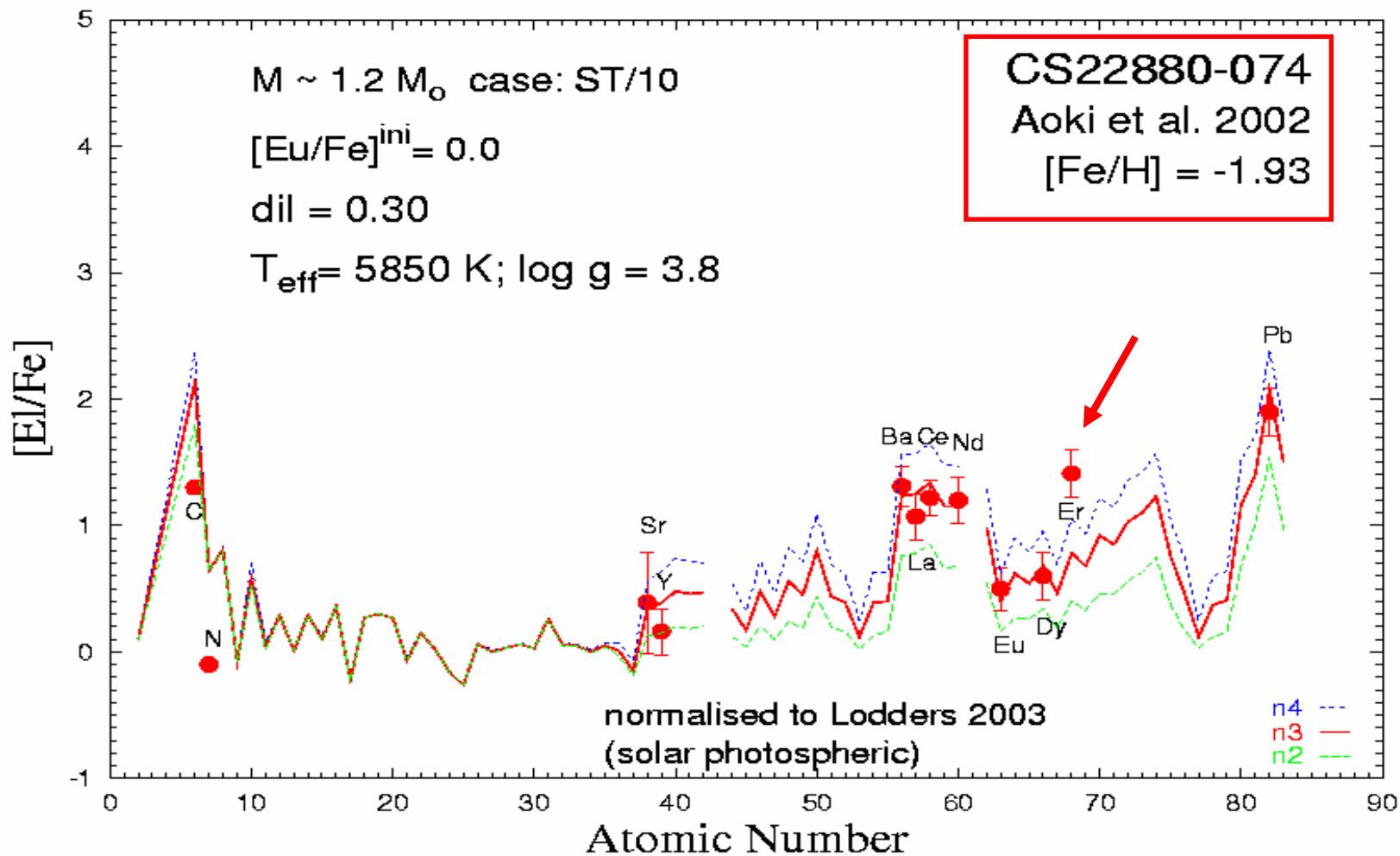
The choice of the initial r-rich isotope abundances normalised to Eu is made considering the r-process solar prediction from Arlandini et al. 1999.

M = 1.5 M sun [Fe/H] = -2.60

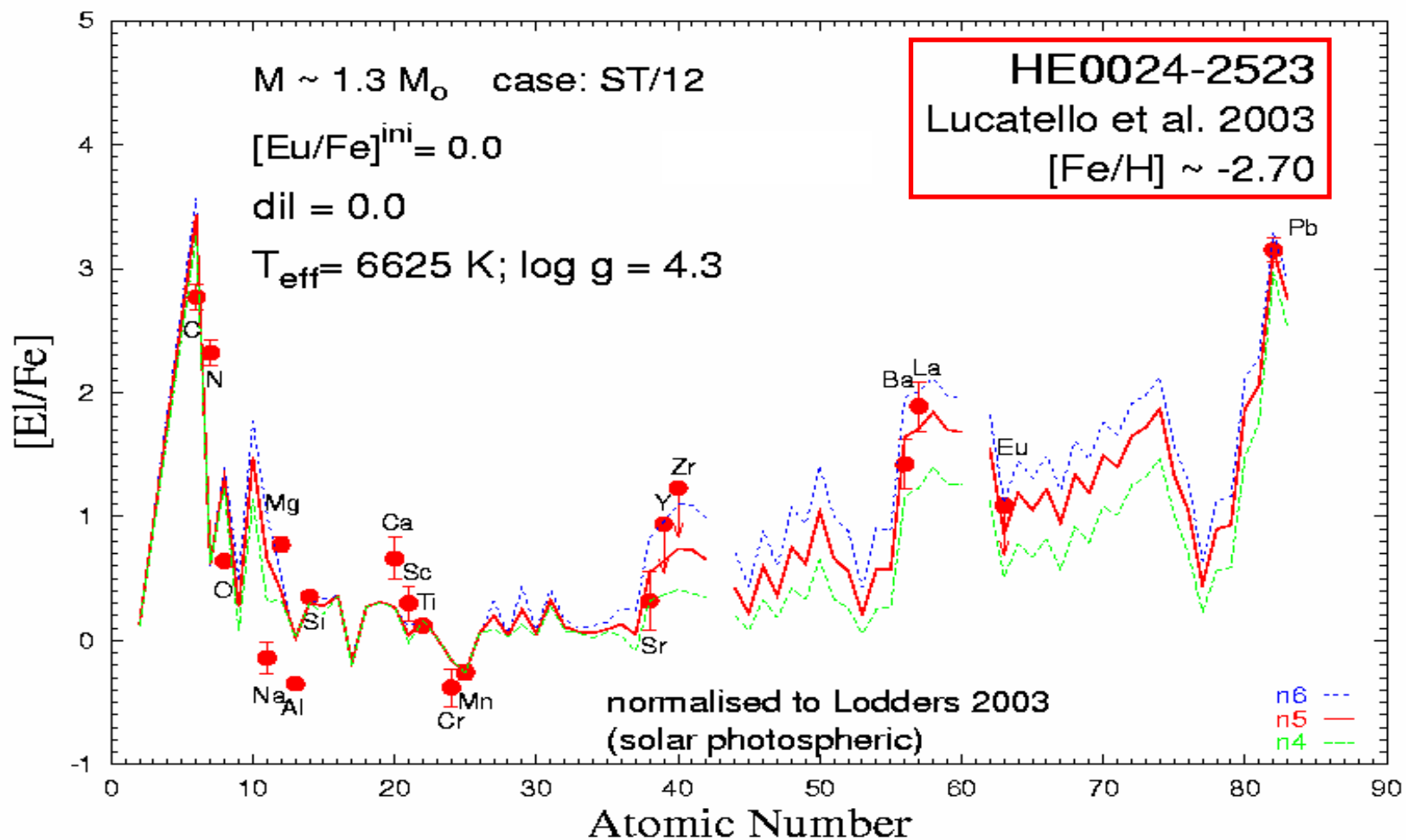
13C pocket	[La/Fe]					[Eu/Fe]				
	norich	rp0p5	rp1	rp1p5	rp2	norich	rp0p5	rp1	rp1p5	rp2
ST	2.16	2.16	2.16	2.17	2.20	1.30	1.34	1.43	1.64	1.99
ST/12	2.76	2.76	2.76	2.76	2.77	1.77	1.79	1.82	1.92	2.14
ST/30	2.08	2.08	2.09	2.11	2.16	0.97	1.04	1.21	1.52	1.94
ST/75	0.76	0.79	0.91	1.14	1.51	0.01	0.44	0.91	1.40	1.90

13C pocket	[La/Eu]				
	norich	rp0p5	rp1	rp1p5	rp2
ST	0.86	0.82	0.73	0.53	0.21
ST/12	0.99	0.97	0.94	0.84	0.63
ST/30	1.12	1.04	0.88	0.59	0.22
ST/75	0.75	0.36	0.00	-0.26	-0.39

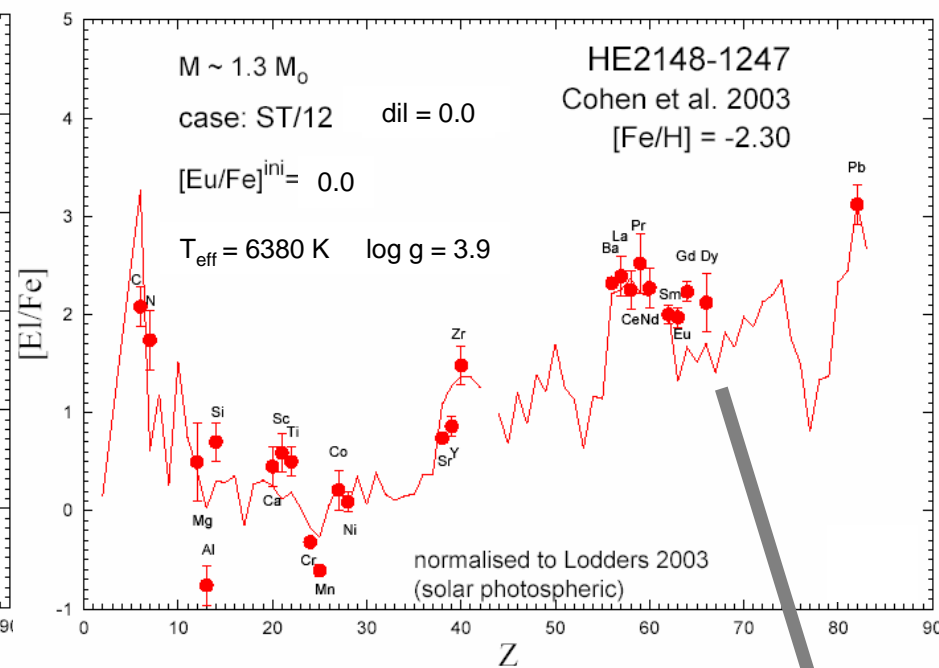
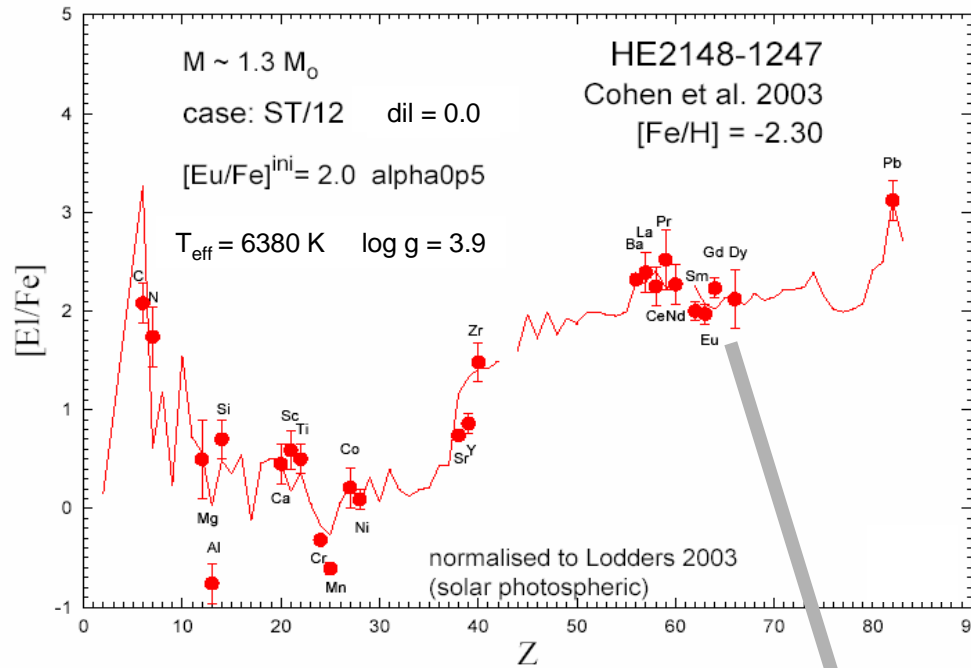
CS 22880-074 Aoki et al. 2002



HE 0024-2543 Lucatello et al. 2003



HE2148-1247 Cohen et al. 2003



With r-process enhancement
→ [Eu/Fe] ini = 2.0

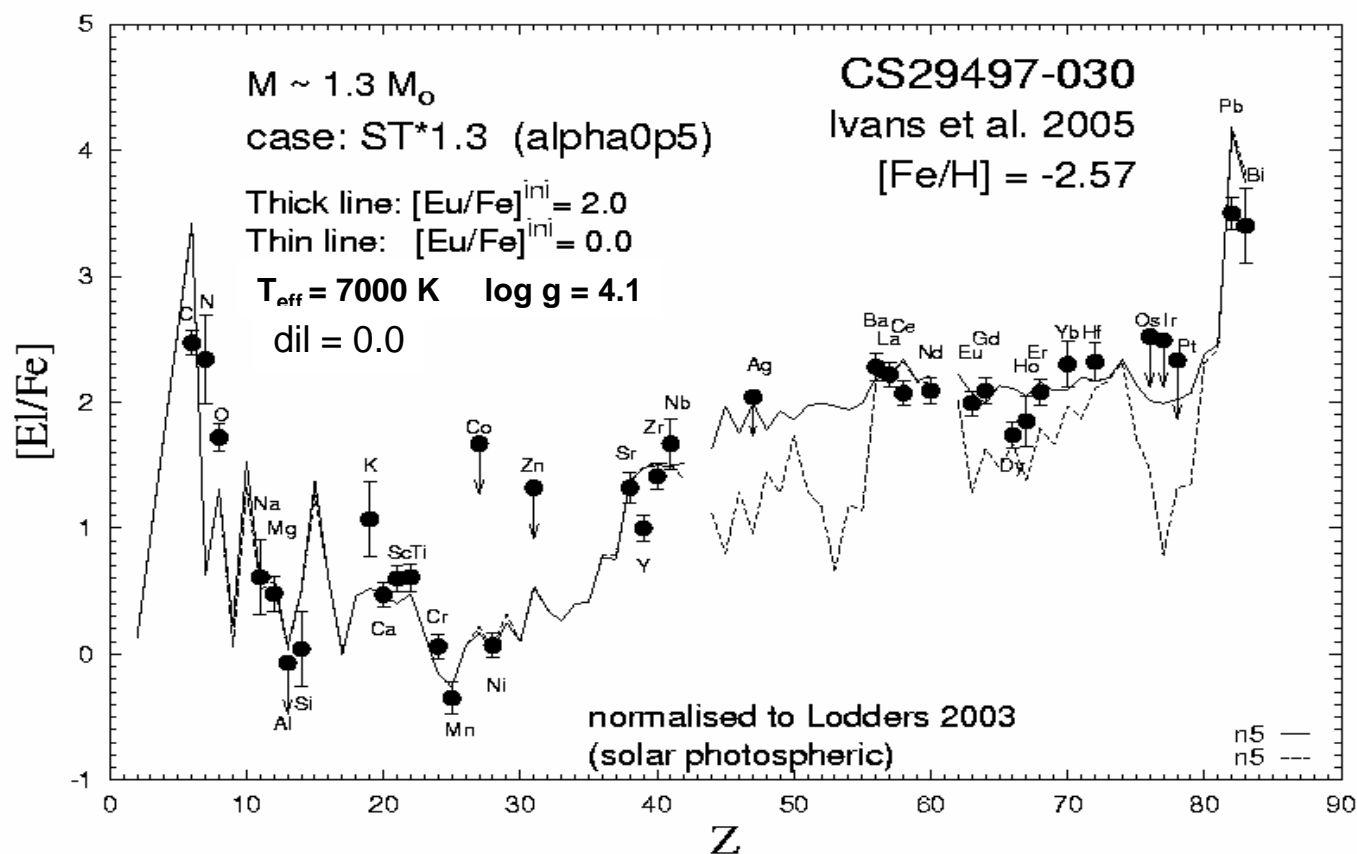
Without r-process
enhancement
→ [Eu/Fe] ini = 0.0

UPDATED

NEAR-ULTRAVIOLET OBSERVATIONS OF CS 29497-030: NEW CONSTRAINTS ON NEUTRON-CAPTURE NUCLEOSYNTHESIS PROCESSES¹

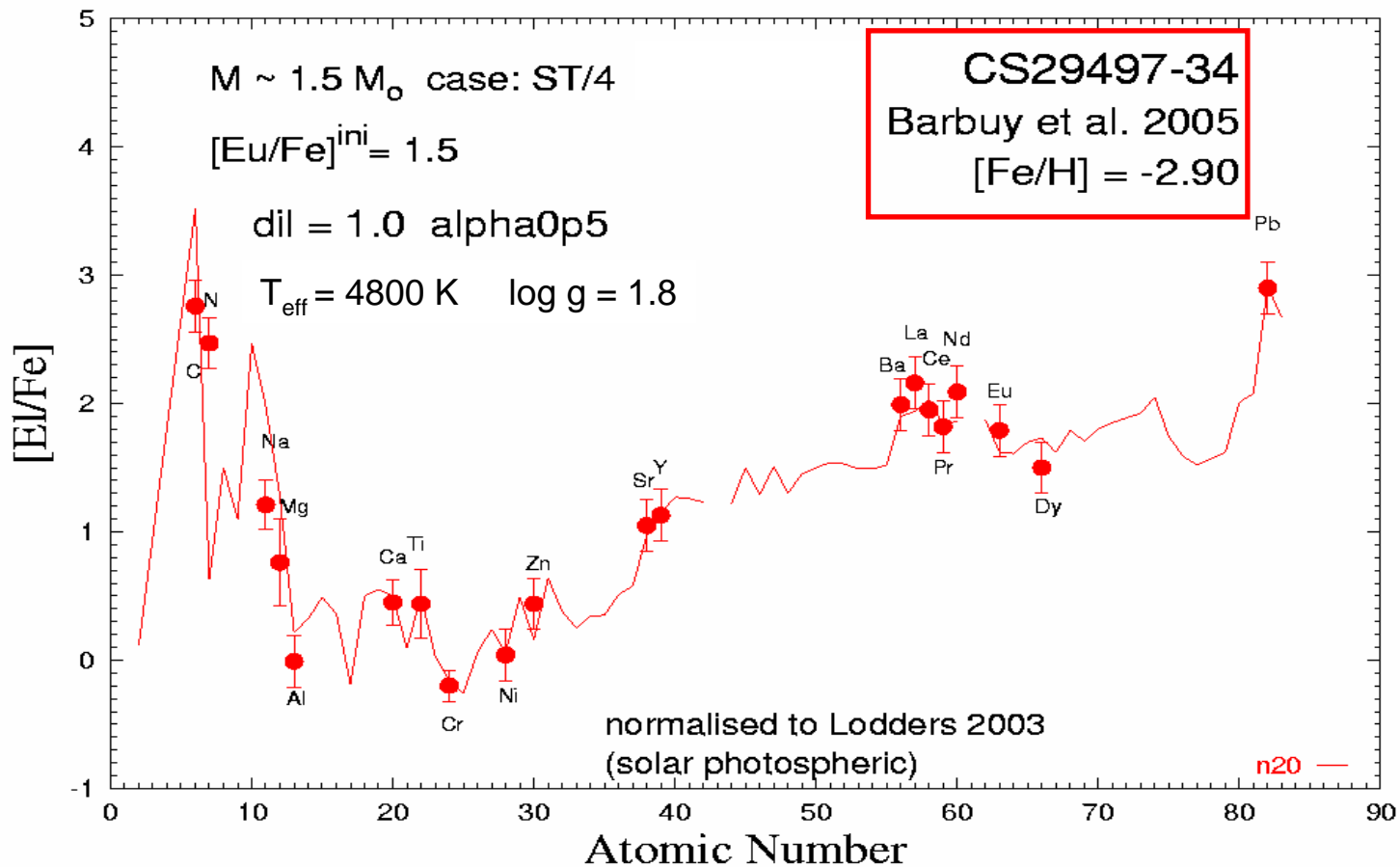
INESE I. IVANS,^{2,3} CHRISTOPHER SNEDEN,⁴ ROBERTO GALLINO,⁵ JOHN J. COWAN,⁶ AND GEORGE W. PRESTON⁷

Received 2005 March 21; accepted 2005 April 28; published 2005 June 28



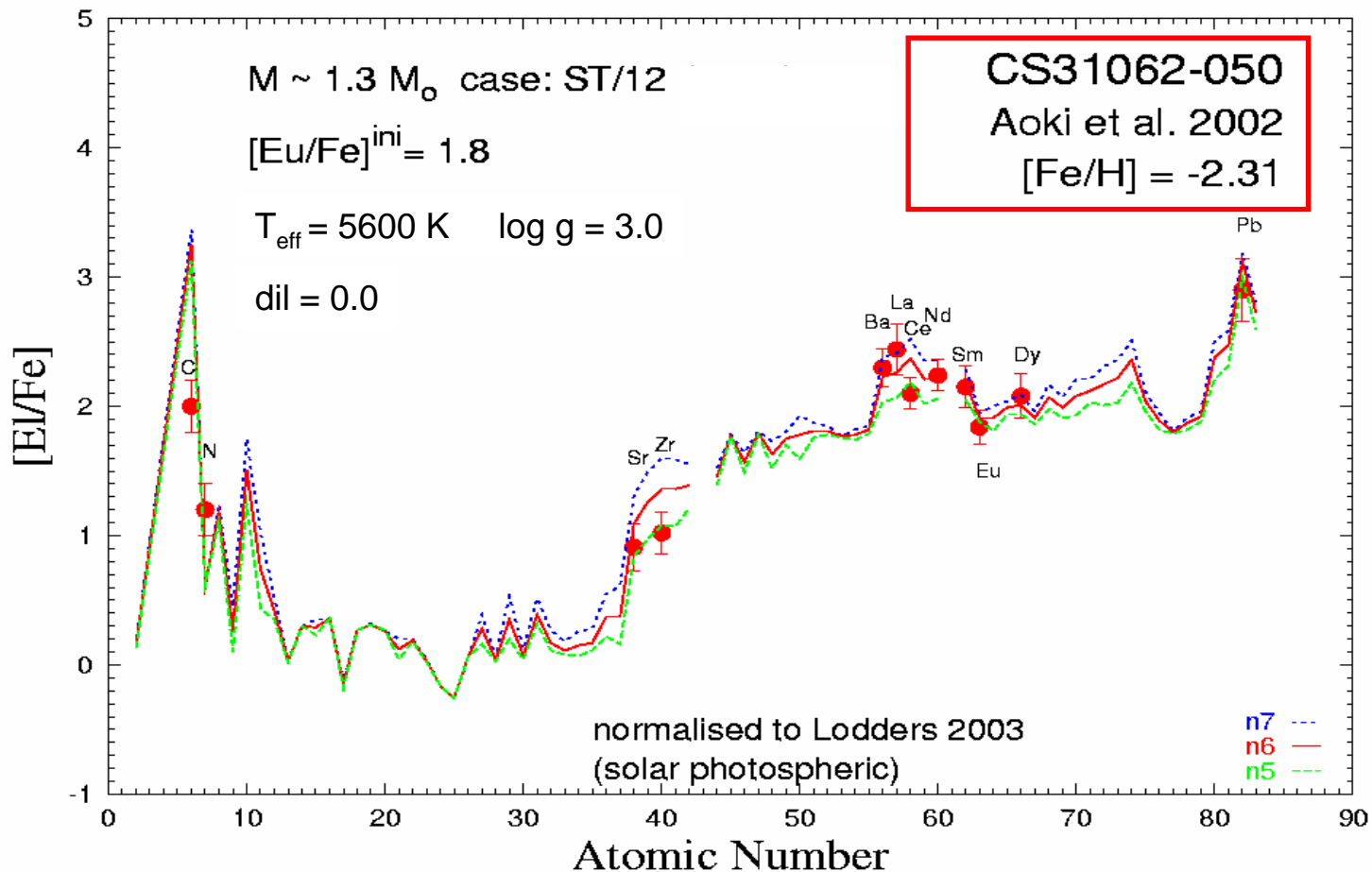
CS29497-34 Barbuy et al. 2005

$$[\text{Eu}/\text{Fe}]^{\text{ini}} = 1.5$$



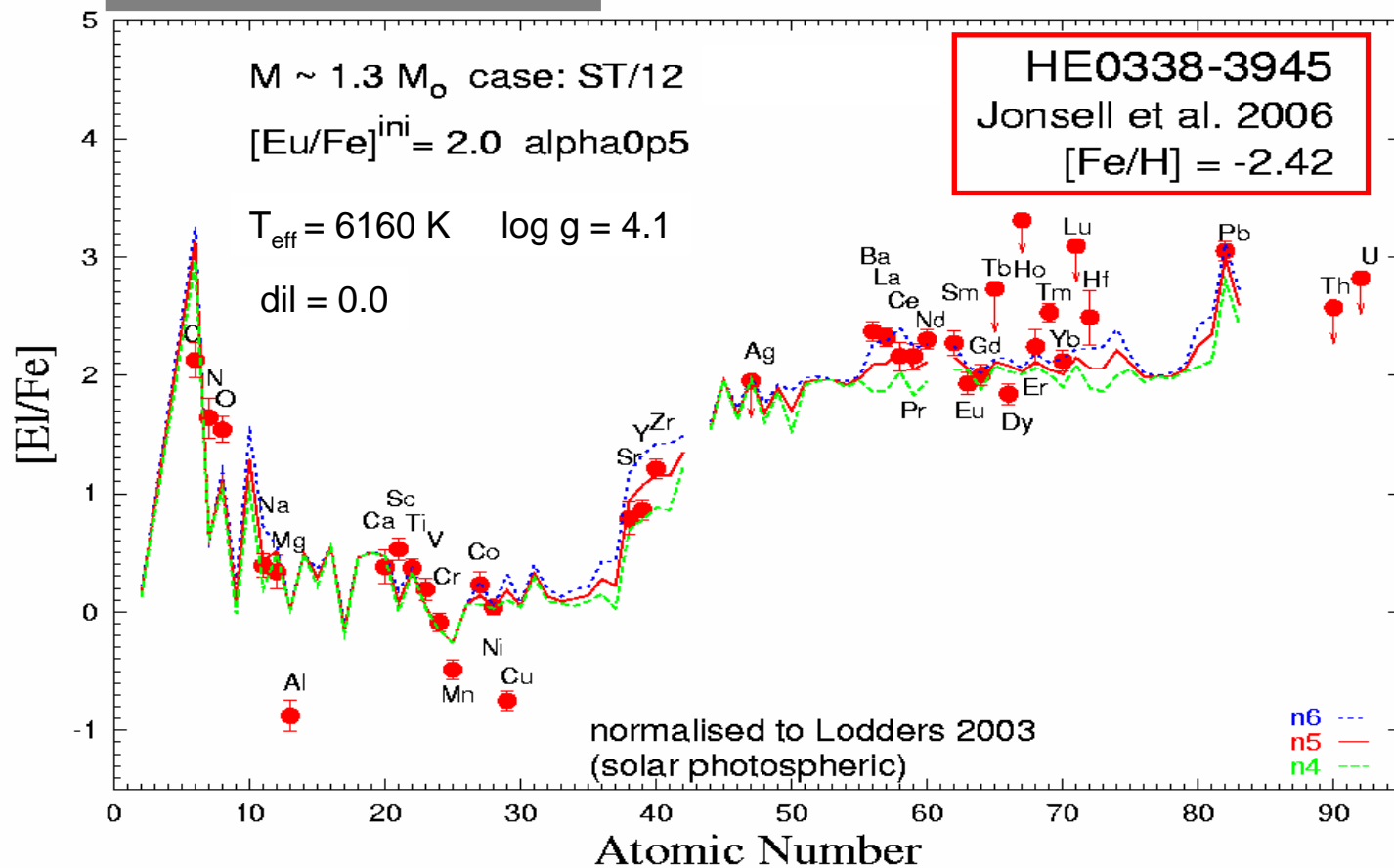
CS31062-050 Aoki et al. 2002

$$[\text{Eu}/\text{Fe}]^{\text{ini}} = 1.8$$



Jonsell et al. astro-ph/0601476

$$[\text{Eu}/\text{Fe}]^{\text{ini}} = 2.0$$



Barklem et al. 2005: s-enhanced stars

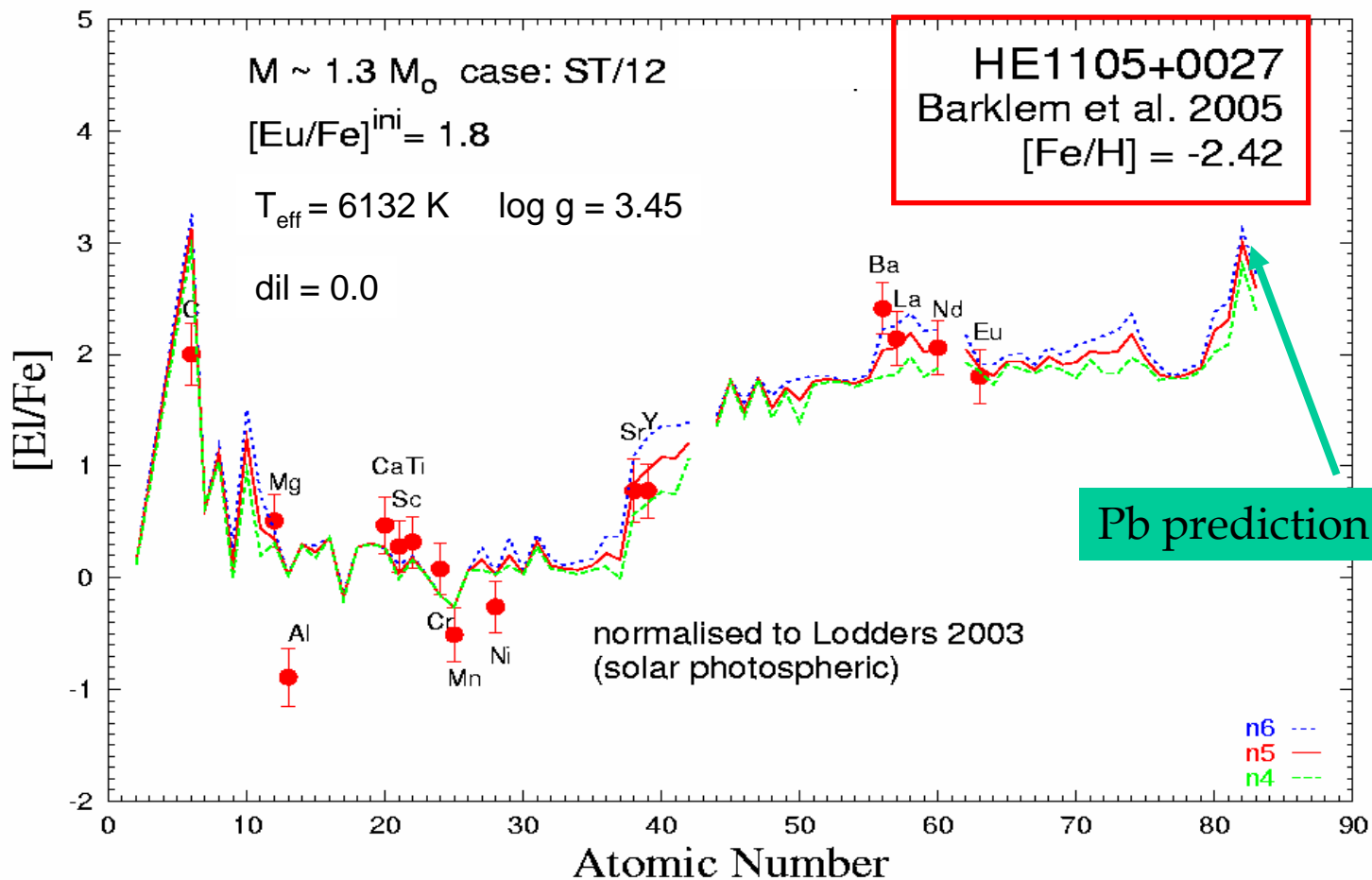
**** our Pb predictions**

C+s-stars	[Fe/H]	T _{eff} (K)	log g	[ls/Fe]	[hs/Fe]	[hs/ls]	M/M _o	¹³ C-pocket	dil	[Eu/Fe]	ref	[Pb/Fe]**	[Pb/hs]**
HE 0202-2204	-1.98	5280	1.65	0.49	1.21	0.72	1.5	ST*1.3	0.90	0.0*	12	3.02	1.82
HE 0231-4016	-2.08	5972	3.59	0.70	1.35	0.65	1.2	ST*1.3	0.00	0.0	12	3.42	2.07
HE 1135+0139	-2.33	5487	1.8	0.51	0.94	0.43	1.5	ST/6	1.85	0.0*	12	1.82	0.88
HE 2150-0825	-1.98	5960	3.67	0.76	1.51	0.76	1.2	ST*1.3	0.00	0.0	12	3.42	1.91
HE 2240-0412	-2.2	5852	4.33	0.24	1.37	1.13	1.3	ST/6	0.00	0.0	12	3.22	1.85
HE 0430-4404	-2.07	6214	4.27	0.58	1.52	0.94	1.2	ST*1.3	0.00	0.0	12	3.42	1.91
HE 0131-3953	-2.71	5298	3.83	0.46	1.97	1.51	1.3	ST/15	0.00	1.5*	12	3.09	1.12
HE 1105+0027	-2.42	6132	3.45	0.74	2.20	1.46	1.3	ST/12	0.00	1.8*	12	3.00	0.80
HE 1430-1123	-2.71	5915	3.75	0.37	1.77	1.40	1.3	ST/15	0.00	0.0*	12	3.09	1.32
HE 2227-4044	-2.32	5811	3.85	0.41	1.33	0.92	1.3	ST/6	0.00	0.0*	12	3.22	1.89

12. Barklem et al., A&A 439, 129 (2005)

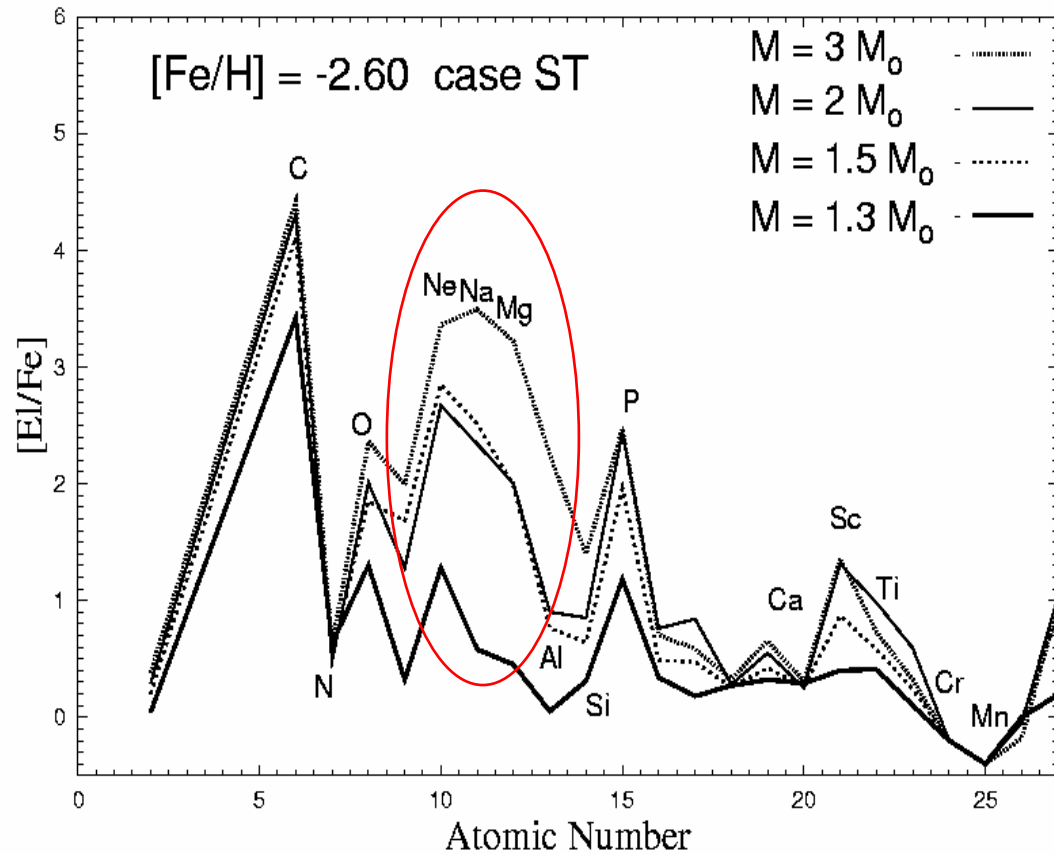
HE 1105+0027 Barklem et al. 2005

$[\text{Eu}/\text{Fe}]^{\text{ini}} = 1.8$

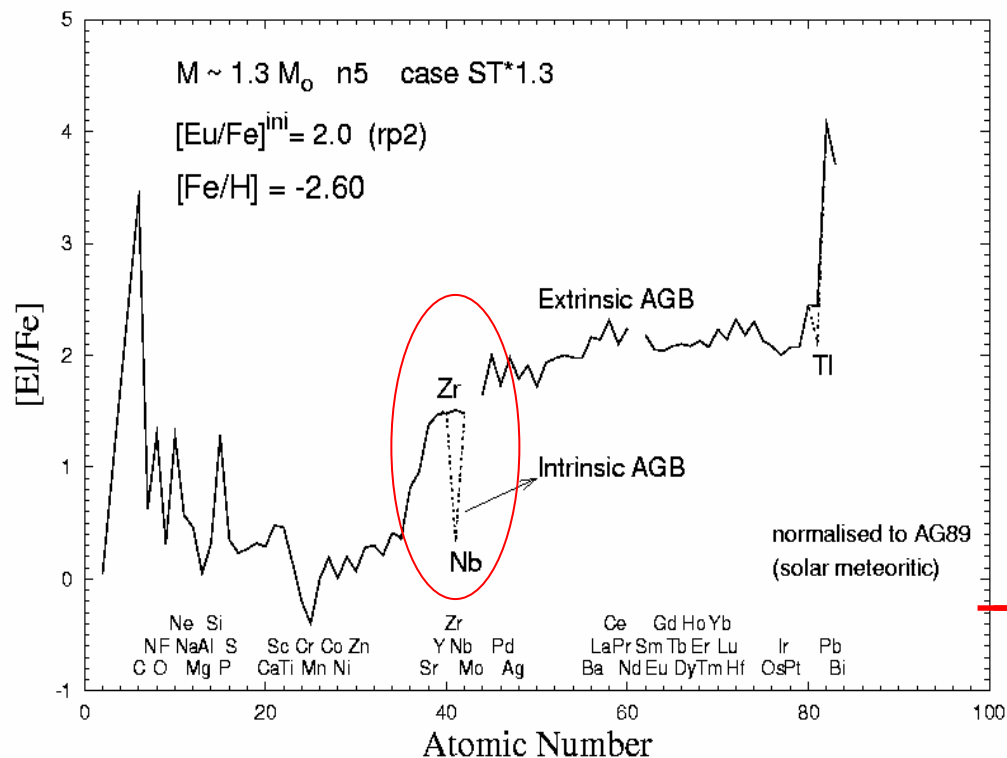


Spectroscopic Na (and Mg) \rightarrow Stellar Mass prediction

AGB models
of $M = 1.3, 1.5, 3 M_{\text{sun}}$
for the same ^{13}C -pocket,
at $[\text{Fe}/\text{H}] = -2.60$.
A strong primary
production of ^{22}Ne
results in advanced
pulses, by conversion of
primary ^{12}C to ^{14}N in the
H-burning ashes
followed by double α
captures on ^{14}N in the
thermal pulse.
This implies a primary
production of ^{23}Na and
 ^{24}Mg via $^{22}\text{Ne}(n,\gamma)^{23}\text{Na}$,
and of
 $^{23}\text{Na}(n,\gamma)^{24}\text{Na}(\beta^-)^{24}\text{Mg}$.



Zr over Nb: Intrinsic or Extrinsic AGBs



Ru 95 1,65 h ϵ : β^+ 1,2... γ 336; 1097; 627... g	Ru 96 5,52 σ 0,25	Ru 97 2,9 d ϵ : γ 216; 324... g	Ru 98 1,88 $\sigma < 8$	Ru 99 12,7 σ 4	Ru 100 12,6 σ 5,8
Tc 94 53 m β^+ 0,8 γ 871; 850... β^+ 2,5... γ 811...	Tc 95 4,9 h 60 d 20 h β^+ 0,8 γ 204; 682; 835... β^+ 1,0 γ 756; 1074...	Tc 96 52 m 4,3 d β^+ 0,8 γ 778; 850; 913... β^+ 1,0 γ 778; 850; 913...	Tc 97 92,2 d 4,0 $\cdot 10^6$ a β^+ 0,4 γ 745; 652 σ 0,9 + 1,67	Tc 98 4,2 $\cdot 10^6$ a β^+ 0,4 γ 745; 652 σ 0,9 + 1,67	Tc 99 6,0 h 10 ⁹ a β^+ 0,3... γ 141... β^+ 0,3... γ 141... β^+ 0,3... γ 141...
Mo 93 6,9 h β^+ 0,8 γ 1477; 685; 263... β^+ 0,8 γ 950...	Mo 94 3,5 $\cdot 10^2$ a σ 13,4	Mo 95 15,92 σ 0,5	Mo 96 16,68 σ 2,5	Mo 97 9,55 σ 0,14	Mo 98 24,13 σ 0,14
Nb 92 10,15 d β^+ 0,5 γ 561; 934...	Nb 93 16,13 a 100 β^+ 0,5 γ 561; 934...	Nb 94 6,26 m 2 $\cdot 10^4$ a β^+ 0,5 γ 871; 703 β^+ 0,5 γ 871; 703	Nb 95 86,6 h 34,97 d β^+ 0,2; 0,9 β^+ 1,0... γ 204...	Nb 96 23,4 h β^+ 0,7... γ 778; 569; 1091...	Nb 97 53 s 74 m β^+ 1,3... γ 658...
Zr 91 11,22 σ 1,2	Zr 92 17,15 σ 0,2	Zr 93 1,5 $\cdot 10^9$ a β^+ 0,06... σ - 2	Zr 94 17,38 σ 0,049	Zr 95 64,0 d β^+ 0,4; 1,1 γ 757; 724... g	Zr 96 2,80 $\cdot 10^{19}$ a β^+ 0,020

s-process path

The s elements enhancement in low-metallicity stars interpreted by mass transfer in binary systems (extrinsic AGBs).

For extrinsic AGBs $[Zr/Nb] \sim 0$. Instead, for intrinsic AGBs $[Zr/Nb] \sim 1$.

The spectroscopic abundances of low-metallicity s- and r-process enriched stars are interpreted using theoretical AGB models (FRANEC CODE), with an initial composition already enriched in r elements from the parental cloud from which the binary system was formed.

- [Zr/Nb] is an indicator of an extrinsic AGB in a binary system: [Zr/Nb] ~ 0 for an extrinsic AGB, [Zr/Nb] ~ -1 for an intrinsic AGB.
- Spectroscopic determination of [Na/Fe] and [Mg/Fe] permits an estimate of the initial AGB stellar mass.

- Open Problem: the strong discrepancy of C and N predictions with respect to observations may be reconciled:

(1) Self consistent production of the ^{13}C -pocket
(Straniero, Cristallo & Gallino 2005, 2006)

(2) Introducing the effect of cool bottom process (CBP)
in the TP-AGB phase (*);

(3) Uncertainties in the spectroscopic abundances of C,
N, O, Na, Mg \rightarrow M. Asplund, ARAA 2005

(*) Nollett, K. M., Busso, M., Wasserburg, G. J., ApJ 582, 1036 (2003);

Wasserburg, G. J., Busso, M., Gallino, R., Nollett, K. M., (2006), Nucl. Physics, in press.